

OPEN ACCESS

EDITED BY Dengrong Sun, Sichuan University, China

REVIEWED BY
Jing Li,
Sichuan University, China
Jinyan Cao,
Kunming University of Science and Technology,
China

RECEIVED 04 September 2025 REVISED 18 September 2025 ACCEPTED 23 October 2025 PUBLISHED 14 November 2025

CITATION

Chen Y, Wen M, Ding T, Fan R, Liu Q, Liu Z and Peng Z (2025) Recent progress in electrochemical decomposition of hydrogen sulfide for sulfur recovery and hydrogen production. *Front. Chem.* 13:1698815. doi: 10.3389/fchem.2025.1698815

COPYRIGHT

© 2025 Chen, Wen, Ding, Fan, Liu, Liu and Peng. This is an open-access article distributed under the terms of the Creative Commons Attribution License (CC BY). The use, distribution or reproduction in other forums is permitted, provided the original author(s) and the copyright owner(s) are credited and that the original publication in this journal is cited, in accordance with accepted academic practice. No use, distribution or reproduction is permitted which does not comply with these terms.

Recent progress in electrochemical decomposition of hydrogen sulfide for sulfur recovery and hydrogen production

Yanjun Chen^{1,2,3}*, Ming Wen^{1,2,3}, Tong Ding^{1,2,3}, Rui Fan⁴, Qisong Liu^{1,2,3}, Zongshe Liu^{1,2,3} and Zicheng Peng⁴

¹Research Institute of Natural Gas Technology, PetroChina Southwest Oil and Gasfield Company, Chengdu, China, ²National R&D Center for High Sulfur Gas Exploitation, Chengdu, China, ³High Sulfur Gas Exploitation Pilot Test Center, China National Petroleum Corporation, Chengdu, China, ⁴PetroChina Southwest Oil and Gasfield Company, Chengdu, China

Hydrogen sulfide (H₂S) generated by industrial processes (such as petroleum refining, natural gas purification, and coal processing) is a highly toxic and corrosive gas, which is detrimental to human health and environment. Electrocatalytic decomposition of H₂S for simultaneous desulfurization and hydrogen production has emerged as a promising approach to addressing environmental pollution whilst achieving valuable utilization of H₂S. Currently, there are two pathways for electrochemical decomposition of H₂S, namely, direct and indirect decomposition. For the direct pathway, H₂S is electrocatalytically oxidized into sulfur at anode using electrocatalysts. However, this approach is hindered by electrocatalyst deactivation due to sulfur passivation. Conversely, the indirect pathway effectively prevents the anodic sulfur passivation by introducing soluble redox couples as mediators, transferring H₂S oxidation reaction from electrode to liquid phase. In this regard, the selection of redox mediators is critical since it affects H₂S oxidation efficiency, sulfur purity, and overall decomposition voltage. In light of the challenges associated with abovementioned electrochemical H₂S decomposition techniques, this review presents recent advancements in strategies to mitigate anodic sulfur passivation for direct decomposition method, as well as the development of redox mediators and process optimization for indirect decomposition method. Meanwhile, a comparative analysis of characteristic and reaction mechanism of both approaches is provided. Finally, perspectives are given on the current challenges and future research directions in the field of electrocatalytic H₂S splitting technology.

KEYWORDS

electrochemistry, direct H_2S decomposition, indirect H_2S decomposition, sulfur recovery, hydrogen production

1 Introduction

 $\rm H_2S$ is a highly toxic and corrosive gas primarily generated from industrial processes such as petroleum refining, natural gas purification, and coal processing (De Crisci et al., 2019; Zheng et al., 2023). Waste gases containing $\rm H_2S$ not only corrode oil and gas pipelines and equipment but also cause environmental pollution and seriously threaten human health

when emitted into the atmosphere (Yu et al., 2024; Zhang et al., 2014). Consequently, the detoxification treatment of H₂S gas is imperative. Currently, most refineries and natural gas purification plants employ the conventional Claus process to convert H₂S into elemental sulfur and water through high-temperature combustion (925-1204 °C) followed by low-temperature catalytic reactions (170-350 °C) (Eow, 2002; Zhang et al., 2015; Zhao et al., 2021). However, this process generates a significant amount of sulfurcontaining tail gas, necessitating additional tail gas treatment units and resulting in an extended process flow (Eow, 2002; Zhao et al., 2021). Moreover, while the Claus process recovers sulfur, it oxidizes valuable hydrogen resources into water, leading to a substantial waste of hydrogen energy. In the context of carbon neutrality and the development of green energy, various strategies have been explored for the simultaneous recovery of sulfur and hydrogen from H₂S, encompassing thermal decomposition, electrocatalytic decomposition, plasma-assisted decomposition, photocatalytic microwave-induced decomposition, and approaches (Basheer and Ali, 2019; Chen et al., 2020; Khabazipour and Anbia, 2019; Li J. et al., 2021; Oladipo et al., 2021; Osasuyi et al., 2022; Sassi and Amira, 2012; Wang S. et al., 2024; Zhang et al., 2024).

Electrochemical decomposition of H₂S demonstrates superior advantages over alternative technologies, featuring mild reaction conditions (room temperature and atmospheric pressure), low energy requirements, high efficiency, simple operation, and spatially separable hydrogen/sulfur products, representing a promising route for clean and value-added H₂S utilization (Yang et al., 2023; Zhou et al., 2018). By constructing a multi-stage electrolysis system, this technology not only enables effective removal of H₂S within a wide concentration range, but also produces green hydrogen and elemental sulfur simultaneously, one-stone-kills-two-birds environmentally friendly and economic benefits (Pei et al., 2021). Electrocatalytic splitting of H2S technology comprises two approaches, namely, direct and indirect H₂S decomposition. The direct electrocatalytic decomposition of H2S occurs at the anode electrode, with a theoretical decomposition voltage (~0.17 V vs. SHE) that is significantly lower than that of water electrolysis (1.23 V) (Kim and Lee, 2023; Zhang et al., 2022). Nevertheless, it faces challenges, including low activity of catalytic materials and sulfur passivation in the sulfur oxidation reaction on electrodes (Yi et al., 2021). In contrast, the indirect decomposition of H₂S employs redox couples as mediators. In this process, sulfur ions are oxidized by redox mediator to elemental sulfur (Zhou et al., 2018). This approach circumvents anode sulfur passivation but encounters issues such as elevated cell voltage and mismatched reaction rates between sulfur oxidation and electrochemical processes; thus, the selection of redox mediators is essential.

Currently, both methods for H_2S decomposition have attracted broad research attention and yielded promising results. In response to the challenges associated with the aforementioned two electrochemical H_2S decomposition technologies, this review summarizes recent research progress on anti-sulfur passivation strategies for direct decomposition method, as well as advancements in redox mediator selection and process optimization for indirect decomposition method. Meanwhile, a detailed comparison is presented between the two methods in

terms of their key characteristics and reaction mechanisms (Figure 1). Lastly, the current challenges and future research directions in the field of electrocatalytic H₂S splitting technology are explored, with the expectation of providing a reference for the research and development of H₂S treatment and resource utilization technologies generated in the purification process of sulfurcontaining natural gas.

2 Direct electrochemical decomposition of H₂S

2.1 Mechanism

The direct electrochemical H_2S splitting involved the sulfide oxidation reaction (SOR) to produce elemental sulfur (Equations 1, 2) at anode and the hydrogen evolution reaction (HER) to produce hydrogen (Equation 3) at cathode (Figure 2a) (Garg et al., 2023). Usually, an alkaline electrolyte was used to dissolve H_2S .

Anode:
$$HS^- + OH^- \rightarrow S + H_2O + 2e^-$$
 (1)

$$S^{2^{-}} \rightarrow S + 2e^{-} \tag{2}$$

Cathode:
$$2H_2O + 2e^- \rightarrow H_2 + OH^-$$
 (3)

The theoretical voltage of directly electrocatalytic splitting of H₂S is lower than oxygen evolution reaction (OER, 1.23 V) in alkaline electrolyte, which is an effective method for the treatment and utilization of H₂S (Figure 2b). However, the deposition of sulfur on the anode during the process creates a passivation layer with extremely high resistivity ($\sim 10^{15} \Omega$ m), which physically obstructs access to the catalytically active sites by sulfide species, resulting in progressive active site deactivation and complete reaction inhibition. Meanwhile, due to the possible existence of various sulfurcontaining oxidation species (polysulfides, 0/-1; element sulfur, 0; sulfite, +4; thiosulfate, -1/+5; sulfate, +6), the sulfur oxidation reaction process in aqueous electrolytes was complex, involving multiple sulfide-containing intermediates and branched-chain reactions (Equations 4-9), which resulted in the complexity of anode reaction products (Anani et al., 1990; Ateya et al., 2003; Kim and Lee, 2023).

$$HS^{-} + (n-1)S + OH^{-} \rightarrow S_{n}^{2-} + H_{2}O; n = 2 \sim 5$$
 (4)

$$S + S_n^{2-} \rightarrow S_{n+1}^{2-}; n = 2 \sim 4$$
 (5)

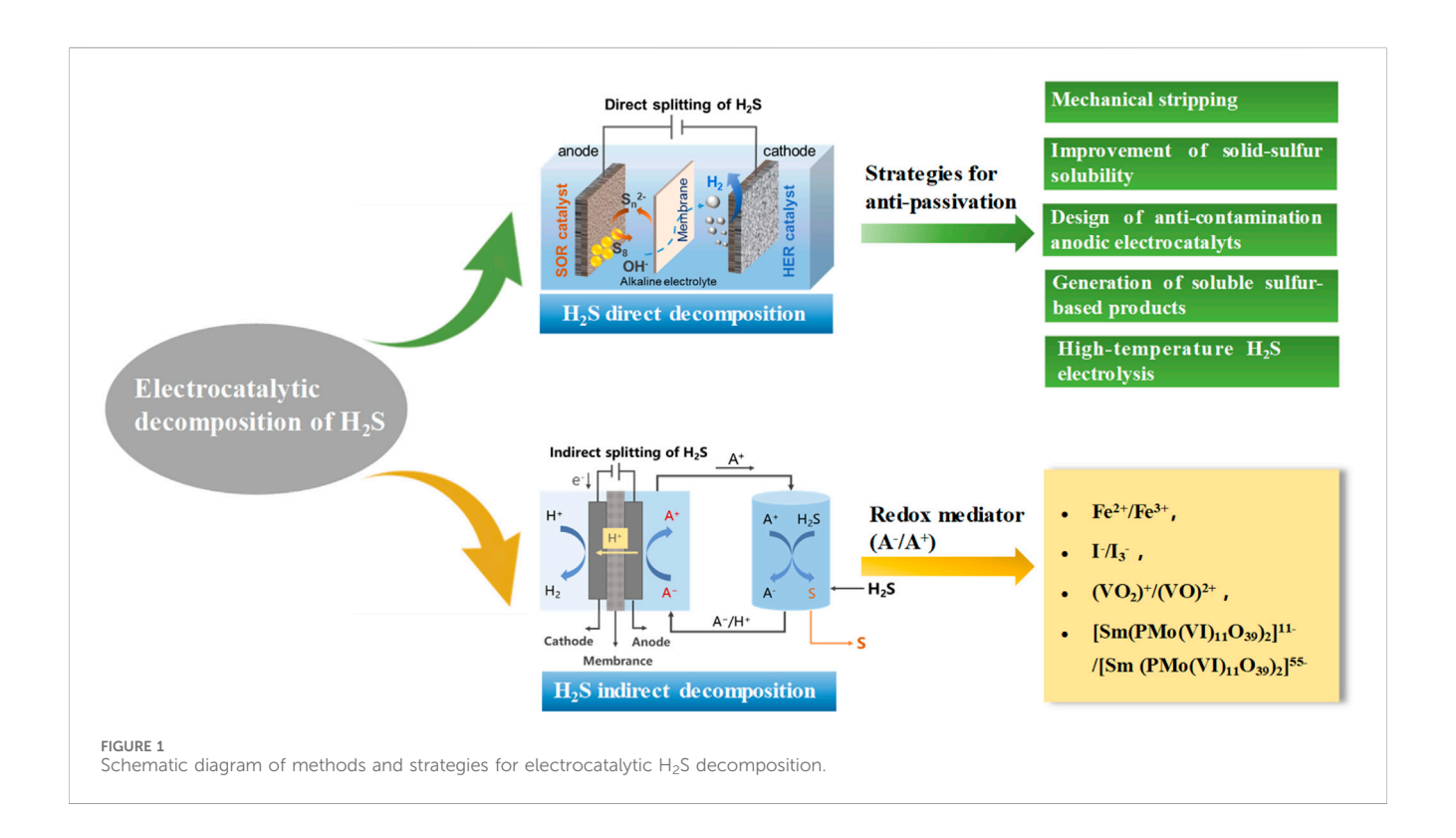
$$2HS^{-} + 8OH^{-} \rightarrow S_2O_3^{2-} + 5H_2O + 8e^{-}$$
 (6)

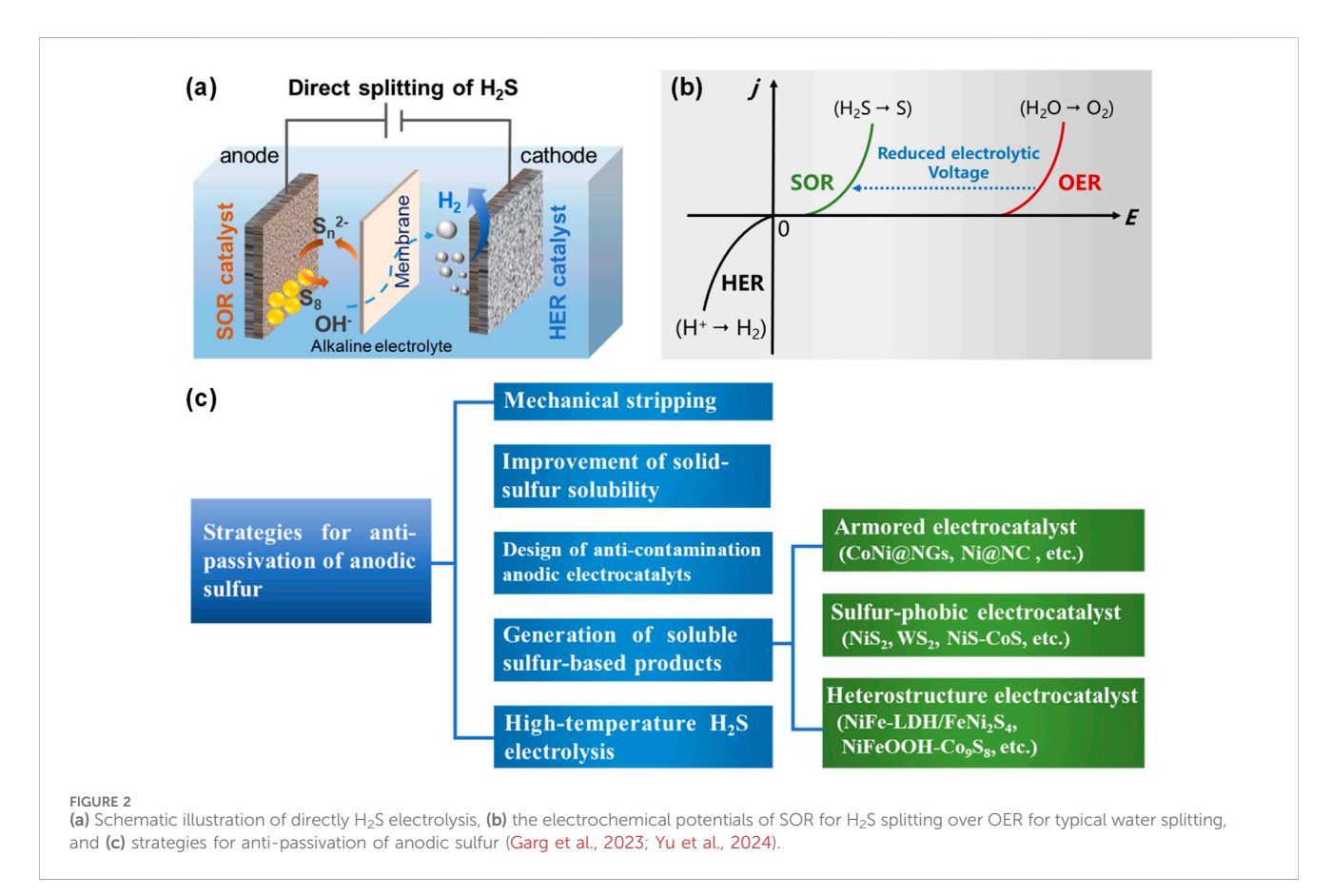
$$S^{2^{-}} + 6OH^{-} \rightarrow SO_{3}^{2^{-}} + 3H_{2}O + 6e^{-}$$
 (7)

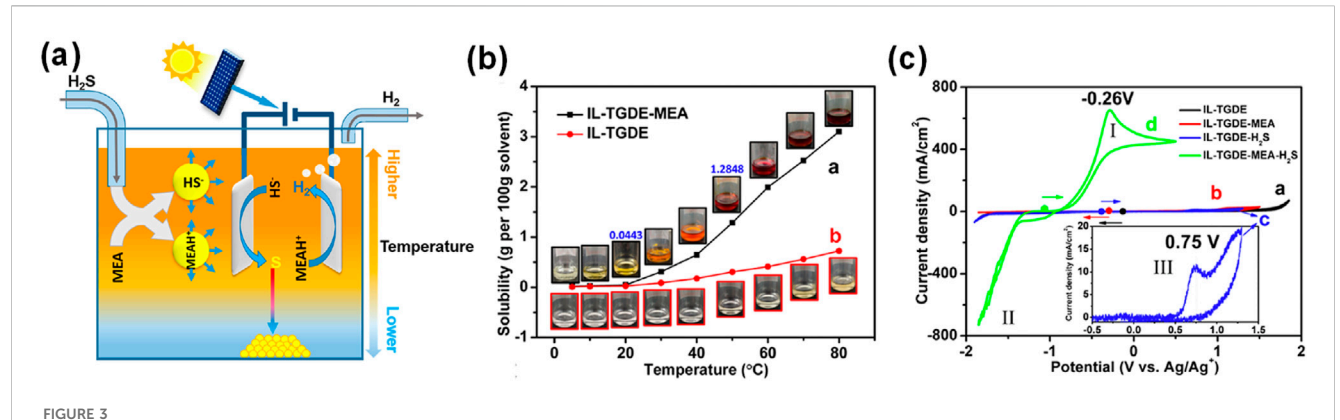
$$S_n^{2^-} + 6OH^- \rightarrow S_2O_3^{2^-} + 3H_2O + (n-2)S + 6e^-; n = 2 \sim 5$$
 (8)

$$S + 4H_2O \rightarrow SO_4^{2^-} + 8H^+ + 6e^-$$
 (9)

To address the issue of anode sulfur passivation, early-stage research primarily focused on employing methods (Figure 2c) such as mechanical stripping and improvement of solid-sulfur solubility to rapidly remove reaction-generated elemental sulfur from the electrode surface, thereby preventing sulfur-induced electrode passivation (Ma et al., 2020; Shih Y S, 1986). In recent years, with the development of catalytic materials and in-depth understanding of the SOR process, researchers have proposed to solve the sulfur passivation problem by designing anticontamination anodic electrocatalyts for SOR (such as armored







Improvement of solid-sulfur solubility. (a) Conceptual schematic of H_2S continuous electrolysis with organic electrolyte system, (b) solubility of sulfur in organic systems for IL-TGDE-MEA and IL-TGDE at different temperatures, and (c) CV curves of a Pt microdisk electrode with a diameter of 30 μ m at 50 °C and a scan rate of 100 mV/s at four organic electrolyte system (Ma et al., 2020).

electrocatalytic materials, sulfur-phobic electrocatalytic materials, etc.) and generation of soluble sulfur-based products (Wei and Wu, 2025; Zhang B. et al., 2021; Zhang et al., 2025). In addition, high-temperature $\rm H_2S$ electrolysis with sulfur being recoverable in gaseous form to prevent solid sulfur deposition at anode has also been developed (Ipsakis et al., 2015).

2.2 Strategies for anti-passivation of anodic sulfur

2.2.1 Mechanical stripping

Mechanical stripping is a method that physically removes the adherents on the surface of the catalyst through external force. The early study demonstrated that the use of mechanical stripping to remove the adhered sulfur at the anode for SOR is feasible. Shih et al. achieved continuous removal of the generated sulfur from the anode by designing the CSTER system (Shih, 1986), a continuously stirred electrochemical reactor, with organic solvent as sulfur dissolver, in which the organic solvent (e.g., toluene or benzene) is mixed with the alkaline sulfide solution by means of continuous stirring to achieve sulfur recovery efficiencies of up to 80% from the anode at ambient temperature and pressure.

2.2.2 Improvement of solid-sulfur solubility

Organic solvents such as ionic liquids used as electrolytes have been demonstrated to have significant potential in enhancing sulfur solubility while maintaining favorable electrical conductivity (Li et al., 2024; Ma et al., 2017; Wang et al., 2019; Yang et al., 2025). Ma et al. constructed an organic electrolyte system for the direct electrolysis of H₂S using ionic liquid [C₃OHmim]BF₄ as the electrolyte, tetraethylene glycol dimethyl ether (TGDE) as the solvent, and monoethanolamine (MEA) as the absorbent for H₂S (Figure 3a). The research finds that the prepared organic electrolyte system is highly temperature-dependent on the sulfur solubility electrolyte and has the catalytic effect of the absorbent MEA. As shown in Figure 3b, due to the solubility of sulfur in organic solutions varying greatly with temperature, the high temperature zone near the anode can maximize the dissolution of precipitated sulfur in the reaction process, and the subsequent low temperature

zone away from the electrode makes the sulfur precipitation, thus recovering sulfur. Meanwhile, the reaction of MEA with H_2S would produce protonated MEA (MEAH⁺) and HS⁻ (MEA + $H_2S \rightarrow$ MEAH⁺ + HS⁻), which not only increases the solubility of H_2S in the electrolyte system, but also makes it easier for H_2S to be electrolyzed into HS⁻ and promotes the oxidation of HS⁻. As a result, the addition of MEA led to a decrease in the oxidation potential of H_2S from 0.75 V to -0.26 V, improving the electrolysis efficiency (Figure 3c). Highly efficient and continuous electrolysis of H_2S can be achieved in this organic electrolyte system with Faraday efficiency of H_2 up to 89%.

2.2.3 Design of anti-contamination anodic electrocatalysts

Designing SOR electrocatalysts with high catalytic activity, antipassivation of sulfur (referring to the ability of the catalyst to prevent sulfur from adhering and causing catalyst deactivation), and longterm stability is an effective strategy to mitigate anodic sulfur passivation in electrocatalytic decomposition of H₂S (Kim and Lee, 2023). Recently, researchers have developed SOR electrocatalysts mainly from the following aspects (Yu et al., 2024): (1) Constructing a sulfur-phobic interface by controlling the catalyst's affinity for sulfur to prevent the product sulfur from adhering to the catalyst surface, facilitating the self-cleaning effect of the electrocatalyst. (2) Modulating the electronic structure of the SOR catalysts by surface modification, alloying, heterojunction construction, and core-shell architecture, could optimize the adsorption and desorption free energies of sulfur-containing intermediates, ensuring the optimum binding between the active catalyst and reaction intermediates, thus improving the catalytic activity while preventing anodic sulfur passivation.

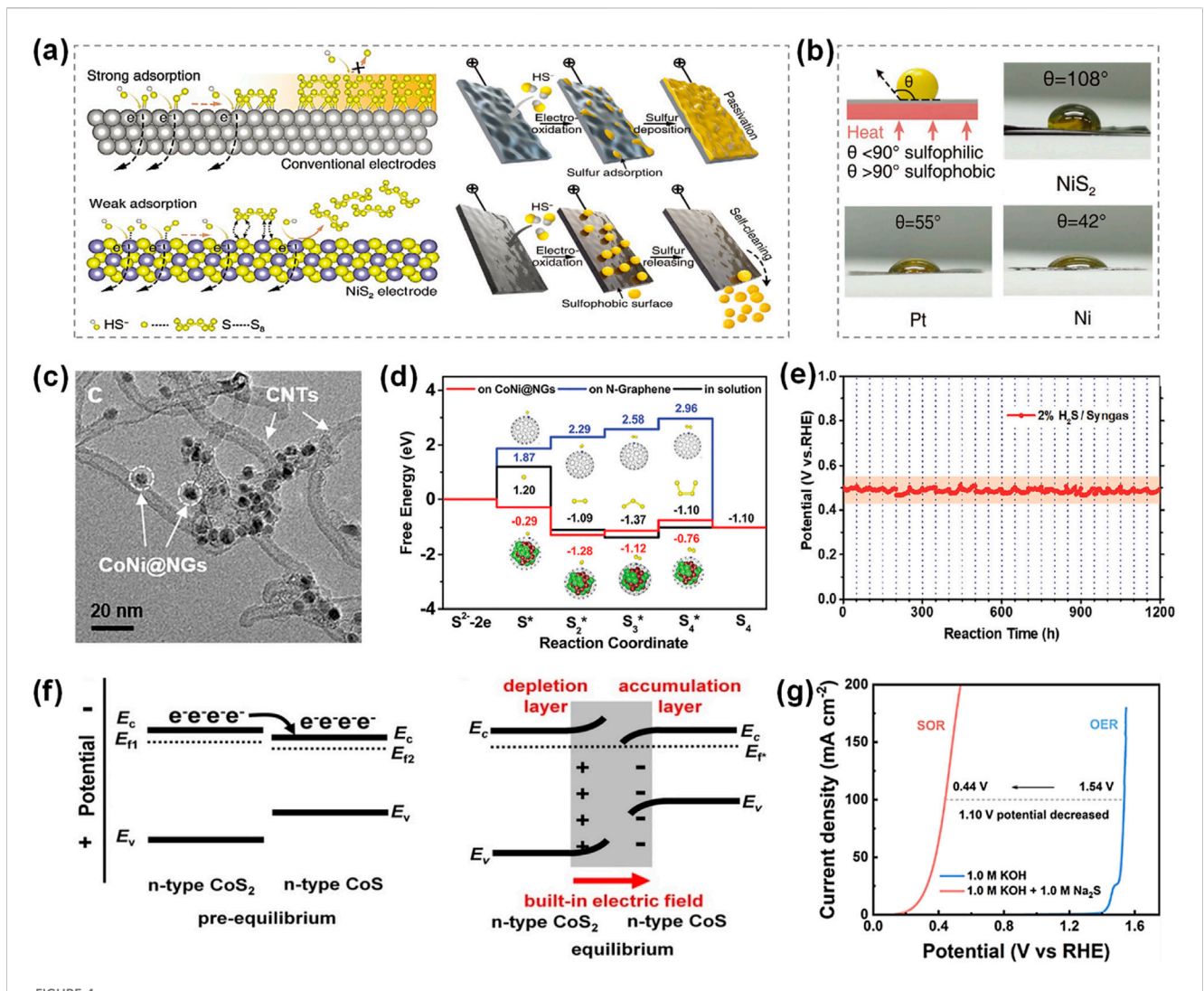
Currently, SOR electrocatalysts include metal oxides, metal sulfides, transition metal selenides/tellurides, metal alloy catalysts, etc. has been reported (Ali et al., 2022; Yu et al., 2024). Table 1 exhibits electrocatalytic performance for recently reported SOR catalysts. Zhang et al. discovered the sulfur-phobic property of transition metal sulfides surface towards sulfur species and developed self-cleaning $\rm NiS_2$ electrocatalysts through a vapor-phase sulfurization method, leveraging sulfur-phobic interface design and controlled sulfur vacancy incorporation (Zhang S.

TABLE 1 Comparison of SOR performance for recently reported catalysts.

Catalyst	Electrolyte	Potential @ 100 mA cm ⁻²	Stability test	Reference
Fe, F-NiO	1 M KOH + 1 M Na ₂ S	0.63 V	100 h@ 1.65 V	Small, 2023, 19, 2302055
Cu ₂ S/NF	1 M Na ₂ S + 1 M NaOH	0.44 V	48 h@ 50 mA cm ⁻²	Green Chem., 2021, 23, 6975
Co ₃ O ₄	1 M Na ₂ S + 1 M NaOH	0.26 V	72 h@ 100 mA cm ⁻²	Adv. Funct. Mater., 2022, 33, 2212183
n-Co ₃ S ₄ @NF	1 M Na ₂ S + 1 M NaOH	0.233V	240 h@ 0.524 V	Nat. Commun., 2024, 15, 6173
Co-Ni ₃ S ₂	1 M Na ₂ S + 1 M NaOH	0.59 V	24 h@ 50 mA cm ⁻²	Chem. Eng. J., 2022, 433, 134472
NiCu-MoS ₂	1 M NaOH	0.35 V	30 h@ 0.3 V	J. Mater. Chem. A, 2022, 10, 13031
Mo-Co-S/NF	1 M Na ₂ S + 1 M NaOH	0.29 V	40 h@ 0.25 V	Inorg. Chem. Front., 2023, 10, 6728
Ni-Co-C/NF	1 M Na ₂ S + 1 M NaOH	0.336 V	64 h@ 100 mA cm ⁻²	Inorg. Chem. Front., 2023, 10, 1447
FeMo-S/Ru	2.43M Na ₂ S +1M NaOH	0.3 V	45 h@ 10 mA cm ⁻²	Adv. Funct. Mater., 2024, 34, 2315326
Co ₃ O ₄ @WS ₂	4 M Na ₂ S + 1 M NaOH	0.6 V	24 h at 10 mA cm ⁻²	J. Mater. Chem. A, 2024, 12, 29184
V _{Pd} -Pd ₄ S MNRs	4 M Na ₂ S + 1 M KOH	0.65 V	20 h@ 10 mA cm ⁻²	Appl. Catal. B Environ., 2024, 340
CoNi@NGs	1 M Na ₂ S + 1 M NaOH	0.52 V	500 h@ 0.317 V	Energy & Environ. Sci., 2020, 13, 119
CuCoNiMnCrS _x	3 M Na ₂ S + 1 M NaOH	0.25 V	120 h@ 1000 mA cm ⁻²	Angew. Chem. Int. Ed., 2024, e202411977
HEA-Mo ₂ C/HPC	1 M Na ₂ S + 1 M NaOH	0.38 V	210 h@ 1000 mA cm ⁻²	ACS Nano, 2023, 17, 25707
NiSe/NF	1 M Na ₂ S + 1 M NaOH	0.49 V	500 h@ 0.4 V	Appl. Catal. B Environ., 2023, 324, 122255
MoSe ₂ /Ni _x Se _y	1 M Na ₂ S + 1 M NaOH	0.5 V	48 h@ 100 mA cm ⁻²	Fuel, 2024, 374, 132532
Ru-CoSe	1 M Na ₂ S + 1 M NaOH	0.273 V	100 h@ 120 mA cm ⁻²	Small, 2024, 20, 2,406,012
NiMoN/MNF	1 M Na ₂ S + 1 M NaOH	0.33 V	100 h@ 300 mA cm ⁻²	Adv. Funct. Mater., 2024, 34, 2407601
NiFe-LDH /Cu-IF	1 M Na ₂ S + 1 M NaOH	0.3 V	120 h@ 50 mA cm ⁻²	Fuel, 2024, 367, 131506

et al., 2021). This NiS₂ catalyst allows for efficient SOR (1.05 g_{sulfur} W h^{-1}) and simultaneous hydrogen production (0.07 g W h^{-1} H₂) with low energy consumption. Theoretical calculations and experimental results demonstrate that NiS₂ is susceptible to the adsorption/desorption of sulfur, ensuring that the generated sulfur will not adhere to the electrode surface (Figures 4a,b). The assembled electrolytic system of H₂S requires an ultralow cell voltage of only 0.65 V to provide a current density of 20 mA cm⁻² and stable operation for more than 100 h. Additionally, similar sulfur-phobic self-cleaning materials such as WS₂ nanosheets prepared by a molten salt-assisted method (Yi et al., 2021) and NiS-CoS nanosheet composites synthesized by a hydrothermal method (Huo et al., 2023) have also been reported.

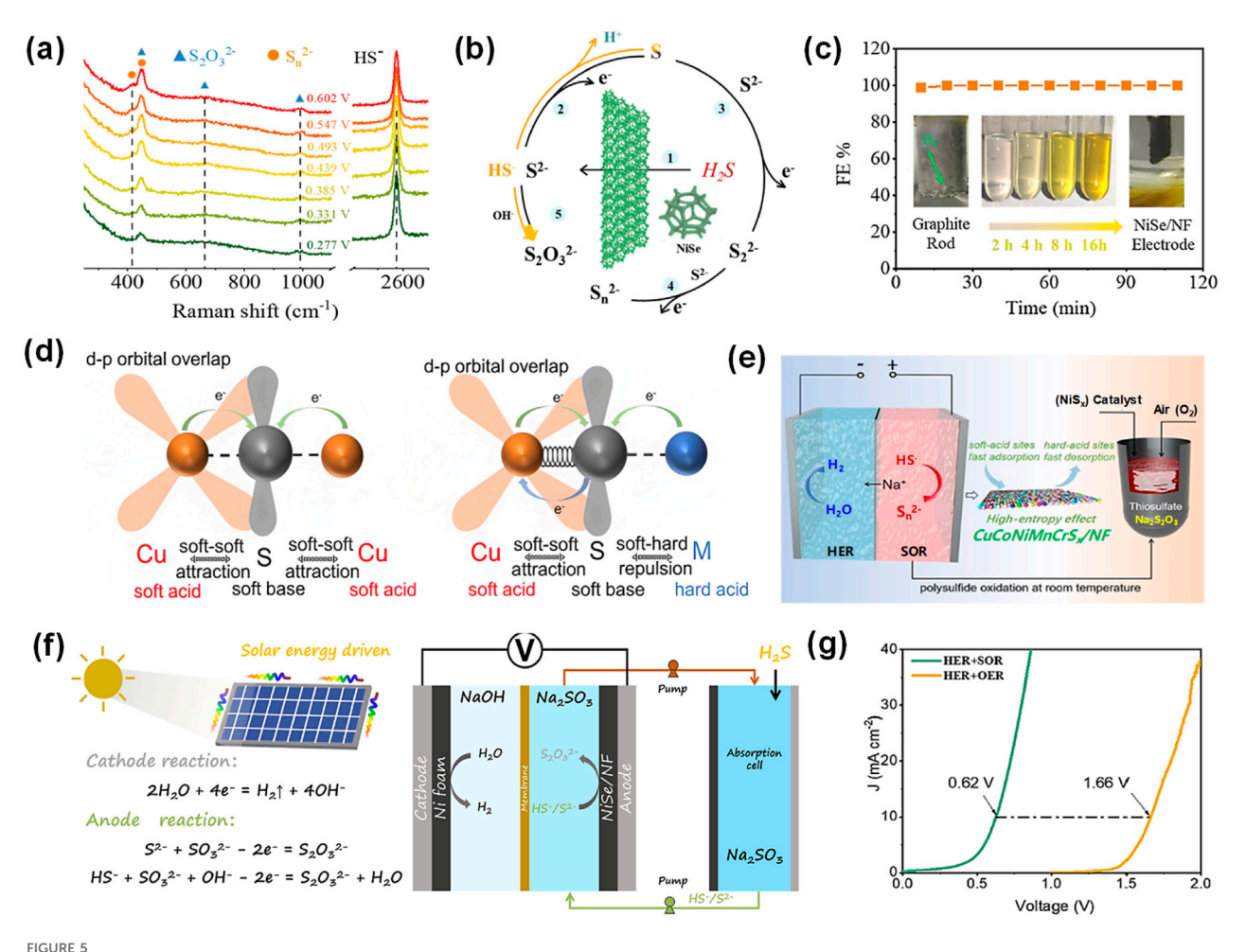
Furthermore, Researchers proposed an armored catalyst strateges such as graphene-encapsulated metal to prevent sulfur passivation (Yu et al., 2022). This approach involves encapsulating transition metal with two-dimensional layered materials, creating well-defined core-shell nanostructures. The two-dimensional layer serves as a protective barrier that effectively prevents electrode corrosion and surface passivation, thereby maintaining catalytic activity. Zhang et al. fabricated a nitrogen-doped graphene-encapsulated non-precious CoNi nanoalloy (CoNi@NGs) by a template-assisted method as the effective electrocatalyst for simultaneous hydrogen and sulfur production from H₂S (Figure 4c) (Zhang et al., 2020). The CoNi@NGs armored catalyst exhibits excellent activity with a potential of 0.25 V for



Design of anti-contamination anodic electrocatalyst. (a) Strong interaction between electrodes and sulfides leads to sulfur passivation during long-term operation, whereas weak interactions repel sulfur and realize self-cleaning electrolysis, and (b) the contact angle measurements of sulfur droplets (120 °C) on NiS₂, Pt and Ni (Zhang B. et al., 2021). (c) HRTEM images of CoNi@NGs armored catalyst, (d) the free energy profiles of the formation of polysulfides (S_x^*) in the aqueous solution on N-Graphene's surface and CoNi@NGs' surface, and (e) durability measurement of CoNi@NGs for removing H₂S in industrial syngas via flowing with 2% H₂S/syngas (Zhang et al., 2020). (f) Schematic diagrams of the energy band structures of the overequilibrium and equilibrium states of the CoS₂/CoS n-n heterojunction, and (g) the LSV curves of NiFe-LDH/FeNi₂S₄/IF (Ma W. et al., 2019).

driving SOR, which is 1.24 V lower than that for OER, suggesting that the energy required to decompose H₂S is much lower than that required to decompose water. Theoretical calculations revealed that the synergy between the encapsulated metal alloy and doped nitrogen modulated the electronic structure of graphene shells, promoting the adsorption of sulfur-containing intermediates (S*) and the formation of polysulfide intermediates on the graphene surface, thus preventing sulfur passivation and inducing high SOR activity (Figure 4d). Meanwhile, the prepared CoNi@NG catalyst was used for the direct electrolysis of H₂S in industrial syngas (49% CO, 49% H₂, and 2% H₂S), which displayed excellent activity and high stability for more than 1200 h at a current density of 20 mA cm⁻² (Figure 4e). Moreover, Zhang et al. reported an integrated electrode with dual-level chainmail structure to facilitate the decomposition of H₂S (Zhang et al., 2025). The primary chainmail is created by a graphene-coated nickel foam skeleton, and the secondary chainmail is formed by graphene-encapsulated nickel nanoparticles. This integrated-chainmail electrode (Ni@NC foam) exhibits an excellent activity and stability for H_2S splitting, which supplies an industrial-scale current density of 1 A cm⁻² at 1.12 V, and can operate stably for more than 300 h at 100 mA cm⁻². Additionally, the Ni@NC foam catalyst realizes the complete removal of 20% H_2S in the simulated crude natural gas (80% CH_4 and 20% H_2S) at the anode to obtain sulfur, and simultaneous acquisition of high-purity hydrogen at the cathode.

The construction of heterostructure is another effective strategy for designing SOR electrocatalysts. The electron redistribution would occur at heterogeneous interfaces due to the Fermi level equilibration between constituent materials, thus modulating the local electronic environment and optimizing the adsorption free energy of sulfur-containing intermediates, thus enhancing the electrocatalytic performance. (Figure 4f) (Ma D. et al., 2019). Ai



Strategies for the generation of soluble sulfur-based products. (a) In situ Raman spectra in the range of 250–2800 cm⁻¹ at a potential between 0.277 and 0.602 V on NiSe/NF electrode in 1.0 M Na₂S and NaOH solution, (b) The schematic diagram of the SOR reaction pathway on NiSe/NF, (c) Hydrogen faradaic efficiencies in galvanostatic test at 100 mA cm⁻² (Duan et al., 2023). (d) Schematic illustration of the Cu-S bonds with/without doping of the hard-acid cations (denoted as M), (e) Schematic illustration of direct H₂S decomposition for yielding Na₂S₂O₃ products (Pei et al., 2024). (f) Direct solar-driven electrochemical decomposition of H₂S to hydrogen and high-value sulfur product, (g) LSV curves of the hybrid HER and SOR of NiSe/NF (Duan et al., 2024).

et al. successfully fabricated heterostructure nanoarrays of NiFe layered double hydroxide (LDH)/FeNi₂S₄ grown on iron foam (IF) substrate (Ai et al., 2024). The obtained NiFe-LDH/FeNi₂S₄/ IF catalyst can effectively catalyze SOR with a low potential of only 0.44 V at 100 mA cm⁻², due to the good hydrophilic surface and the good heterojunction interface (Figure 4g). Semwal et al. developed NiFeOOH-Co₉S₈ intercalated nanostructure arrays with varying Fe: Co ratios grown on nickel foam (NF) substrate by one-step method at low-temperature (50 °C) (Semwal et al., 2023). The NiFeOOH-Co₉S₈ heterojunction catalyst required only 0.84 V to achieve an industrial-grade current density of 1 A cm⁻² in the coupled SOR-HER system. Jin et al. reported the synthesis of terephthalic acid (TPA)-anchored Ni₃S₂ (TPA-Ni₃S₂) brush-like nanoarrays on NF substrate (Jin et al., 2022). The introduction of TPA ligands facilitated the formation of a unique nanorod @nanosheet interfacial structure, which not only modulated the electronic structure of Ni₃S₂ to optimize the adsorption strength of sulfurcontaining intermediates but also increased the number of active sites, thereby enhancing the catalytic performance for SOR.

2.2.4 Generation of soluble sulfur-based products

Recent studies demonstrate that the products distribution of anodic SOR in electrocatalytic decomposition of H2S can be precisely controlled by optimizing key operational parameters, including applied potential window and electrolyte pH, in conjunction with rational electrode material design. Soluble sulfur-based products for SOR can be obtained through the tailored reaction pathway, effectively alleviating anodic sulfur passivation. The distribution of sulfur-based products at anode is intrinsically linked to the reaction mechanism of SOR. However, the mechanistic understanding of the SOR during the electrocatalytic decomposition of H2S remains incomplete. To address the complexity of SOR mechanisms on electrode materials, Duan et al. successfully constructed NiSe2/NF nanoarrays on nickel foam (NF) via a hydrothermal method for electrocatalytic H2S decomposition (Duan et al., 2023). By employing in situ characterization techniques, including Fourier-transform infrared spectroscopy and Raman spectroscopy, they elucidated the sulfur ion oxidation pathway (Figure 5a). When employing 1 mol/L

NaOH-Na₂S solution as the H₂S absorbent, the selective conversion of HS⁻/S²⁻ to polysulfides (S_n^{2-} , n > 2) and the byproduct $S_2O_3^{2-}$ rather than elemental sulfur was achieved (Figures 5b,c), effectively preventing electrode sulfur passivation during prolonged operation. Subsequently, the electrochemically generated polysulfides were converted to elemental sulfur through acidification in an ice bath using concentrated sulfuric acid. The experimental results show that the NiSe₂/NF catalyst can operate stably for 500 h at 0.49 V. Additionally, Yang et al. systematically investigated Ni as the anode material for SOR (Yang et al., 2019). Their studies revealed that significant sulfur passivation occurred at the anode, during H₂S electrolysis in Na₂HPO₄ solution (pH 9.2), In contrast, when operated in strongly alkaline media (pH 13), the formation of passivating sulfur layers was effectively suppressed. These results demonstrate that a higher pH condition preferentially inhibits sulfur passivation.

Furthermore, Pei et al. developed an amorphous high-entropy sulfide catalyst of CuCoNiMnCrSx nanosheets for SOR, which provided a current density of 100 mA cm⁻² at an ultra-low potential of 0.25 V, and maintained stable operation for 100 h at an industrial-grade current density of 1 A cm⁻² (Pei et al., 2024). The superior SOR performance is attributed to the tailored chemical environment around Cu+ sites by soft/hard metal cations and the designed "soft acid" (Cu+) to "hard acid" (Co2+/Ni2+, Mn2+/Cr3+) active sites, which synergistically promote sulfur adsorption/ desorption and facilitate the efficient conversion of S^{2-} into S_n^{2-} , preventing sulfur passivation at anode (Figure 5d). Particularly, this work designed an electrochemical-chemical tandem oxidation strategy to further convert S_n²⁻ into higher-value thiosulfate over NiS_x catalyst (Figure 5e). Subsequent concentration, filtration, and crystallization yield high-purity sodium thiosulfate pentahydrate crystals (Na₂S₂O₃·5H₂O). This approach effectively circumvents the economic limitation of conventional acidification-based sulfur precipitation recovery.

Additionally, Duan et al. proposed a strategy for directional control of SOR products through adding reaction medium (Duan et al., 2024). The S²-/HS⁻ can be oxidized into high-valued Na₂S₂O₃ via a one-step method using NiSe as catalyst in Na₂SO₃ media solution (Figure 5f), which effectively avoids sulfur passivation and complex sulfur recovery, achieving a current density of 200 mA cm⁻² at a lower potential of 0.66 V (Figure 5g). The reaction pathway was verified by *in situ* Fourier-transform infrared spectroscopy and Raman spectroscopy, which provided real-time monitoring evidence for the following surface electrochemical reactions (Equations 10, 11):

$$2HS^{-} + SO_{3}^{2-} \rightarrow S_{2}O_{3}^{2-} + H^{+} + 2e^{-}$$
 (10)

$$S^{2^{-}} + SO_{3}^{2^{-}} \rightarrow S_{2}O_{3}^{2^{-}} + 2e^{-}$$
 (11)

2.2.5 High-temperature H₂S electrolysis

Except for aqueous electrolytes, high-temperature solid electrolyte cells for the decomposition of H_2S have also been initially developed. H_2S -containing gas is oxidized at the anode of a high-temperature solid molten electrolyte cell to obtain sulfur and protons, in which sulfur is discharged in the form of sulfur vapor from the anode chamber at high temperature, and then cooled and concentrated to collect sulfur at the outlet, thus preventing

sulfur from being enriched at the anode electrode and prompting continuous anodic reaction (Ipsakis et al., 2015). Meanwhile, protons go through the solid electrolyte membrane to reach the cathode chamber, being reduced to hydrogen. The reported protonconducting solid electrolytes include LiSO₄, CsHSO₄, (ZrO₂)_{0.92}(Y₂O₃)_{0.08}, Y-CeO₃, BaCeO₃, etc. (Yates and Winnick, 1999; Chuang, et al., 2000; M. Liu et al., 2001; Sezer et al., 2020). Mbah et al. synthesized a RuO2-CoS2 nanocomposite as an efficient anode catalyst for electrochemical H₂S decomposition (Mbah et al., 2010). They assembled an H₂S decomposition cell employing CsHSO₄ as a high-temperature molten solid-state electrolyte (Figure 6a). Remarkably, under optimized conditions of 150 °C and 1.35 bar where sulfur viscosity was minimized, the system could achieve the electrolytic splitting of H₂S (100% content) (Figure 6b). The high-temperature solid electrolyte cells could exhibit exceptional H₂S decomposition efficiency, due to the high ionic conductivity of the molten electrolyte, accelerating the electrochemical reaction kinetics. Furthermore, this approach facilitates the efficient separation of the obtained hydrogen and elemental sulfur, with sulfur being recoverable in gaseous or liquid form, thus preventing electrode blockage caused by solid sulfur deposition.

Although strategies such as modulating reaction process parameters, selecting appropriate organic solvents as electrolytes, and designing SOR catalytic materials have partially addressed the sulfur passivation of electrode in the direct electrocatalytic decomposition of $\rm H_2S$, challenges such as the susceptibility of electrode materials to sulfidation at high current density, poor material stability, and low sulfur recovery efficiency still persist. Furthermore, due to the complex forms of sulfur in different electrolytes and the diverse existence of SOR products, the obtained sulfur species are complex. The targeted modulation to obtain a single sulfur-based chemical product is crucial for the valorization of sulfur resources and represents a pivotal step toward the industrial application of this technology.

3 Indirect electrochemical decomposition of H₂S

3.1 Mechanism

The indirect electrocatalytic facilitation of the H₂S splitting into hydrogen and elemental sulfur was achieved by means of redox mediators in two consecutive steps: absorption oxidation and electrocatalytic regeneration (Figure 7a) (Zhou et al., 2018). In the absorption reactor (Equation 12), the oxidized-state mediator (A⁺) in the liquid absorbent solution oxidizes H₂S into elemental sulfur, while being reduced to its reduced-state mediator (A-). During the electrochemical regeneration, the reduced-state mediator is converted into a reusable oxidized form at anode, while hydrogen products are obtained at the cathode (Equations 13, 14). Compared to the direct electrocatalytic decomposition of H2S, the anodic sulfur passivation can be fundamentally prevented in redox-mediated H₂S splitting, due to the sulfur precipitation occurring at absorption reactor rather than on the electrode, simultaneously achieving the recycling of redox mediator.

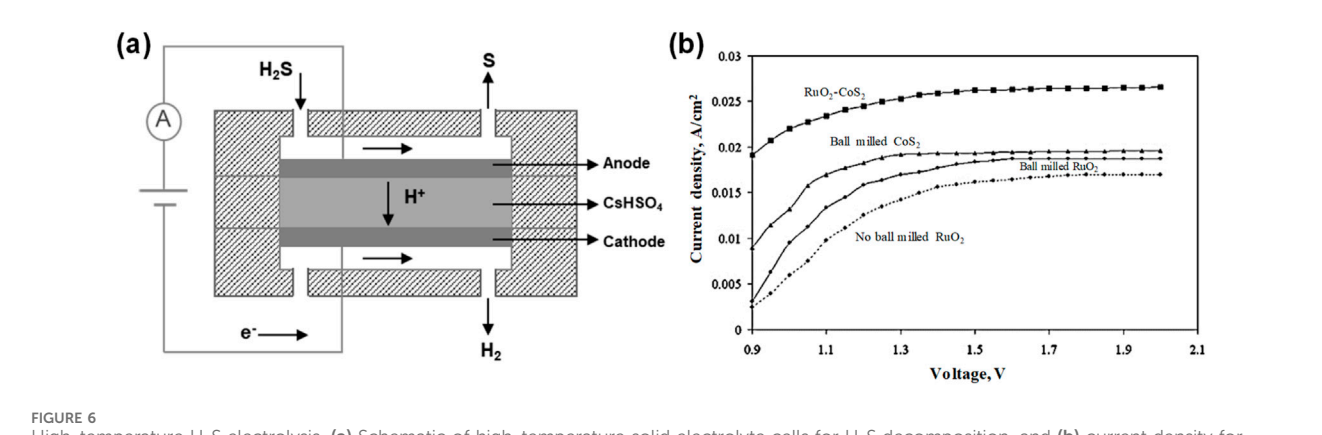
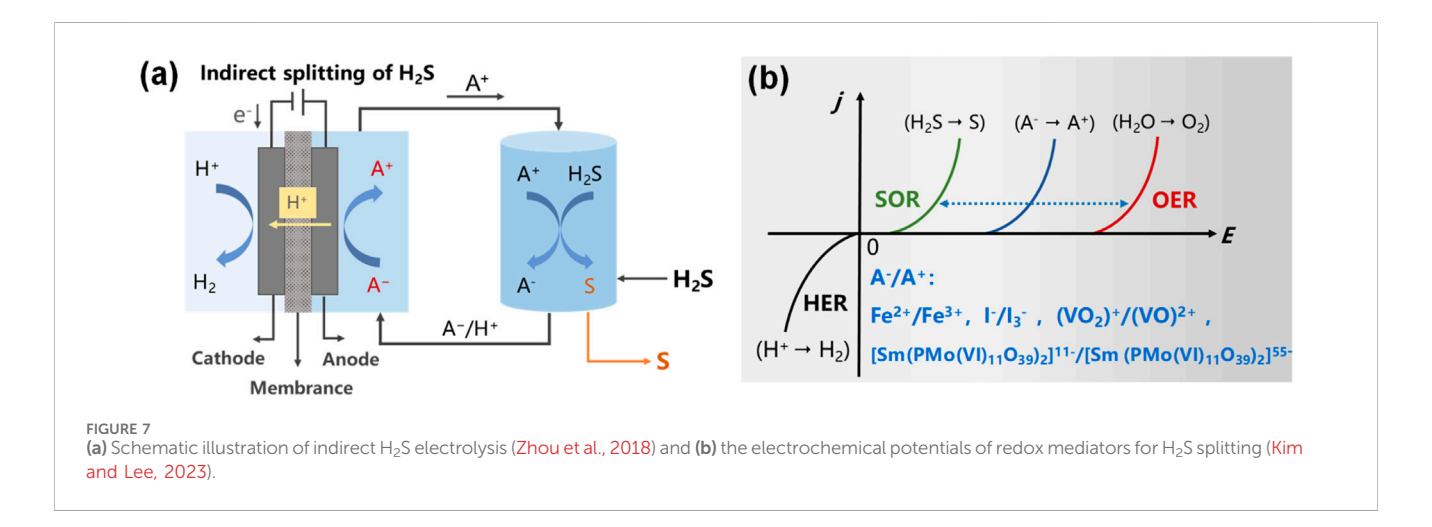


FIGURE 6
High-temperature H₂S electrolysis. (a) Schematic of high-temperature solid electrolyte cells for H₂S decomposition, and (b) current density for different anode configurations with 100% H₂S feed gas content (Mbah et al., 2010).



Oxidation of
$$H_2S: A^+ + H_2S \rightarrow A^- + 2H^+ + S \downarrow$$
 (12)

Oxidation at anode:
$$A^- - 2e^- \rightarrow A^+$$
 (13)

Reduction at cathode:
$$2H^+ + 2e^- \rightarrow H_2 \uparrow$$
 (14)

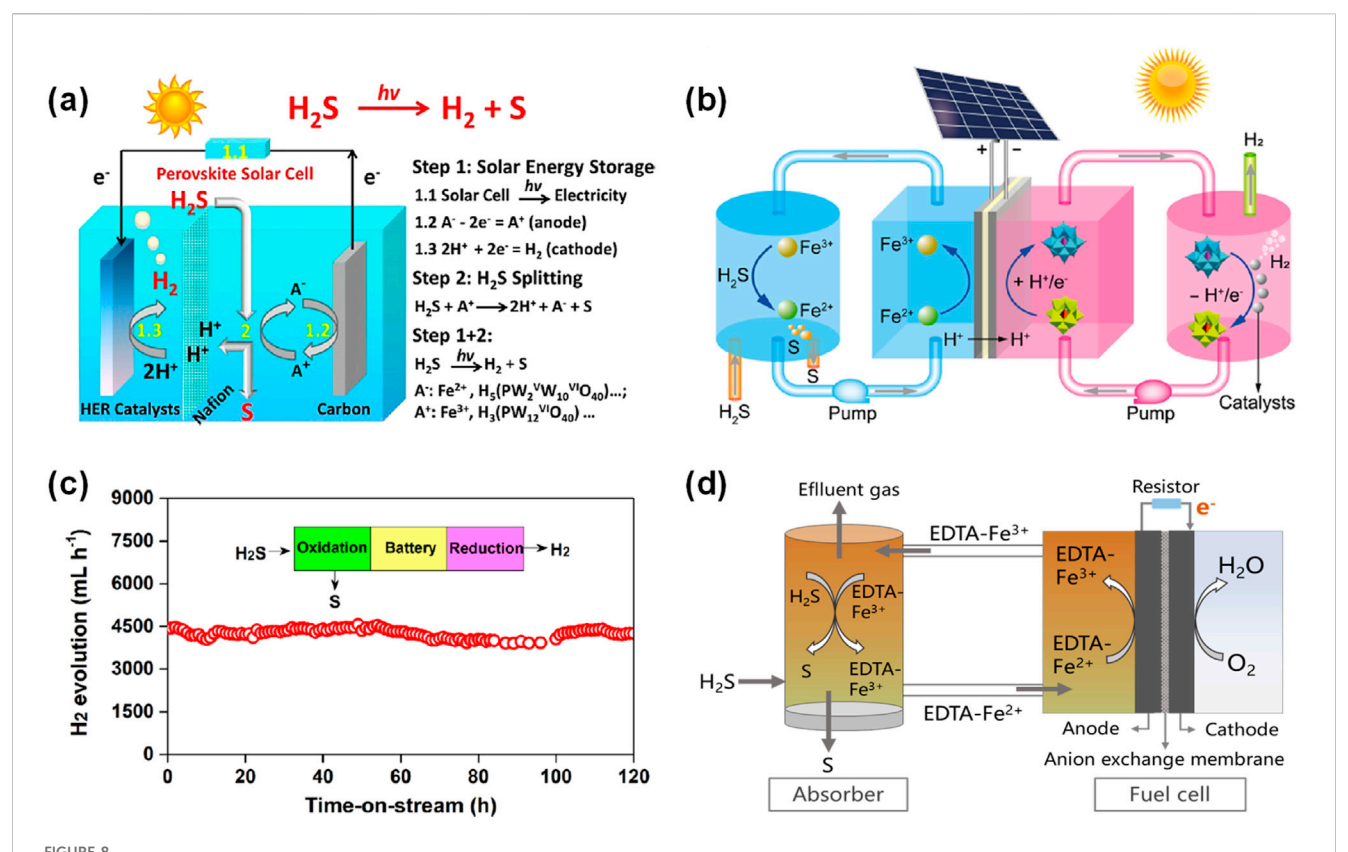
where A⁻ and A⁺ are the reduced and oxidized states of the redox mediator, respectively.

In the indirect electrocatalytic decomposition of H₂S system, the selection of a redox mediator is of paramount importance as it governs two key process parameters: H₂S conversion efficiency and elemental sulfur purity. Generally, the selection of a redox mediator should satisfy the following criteria: (1) The redox medium must possess an appropriate redox potential (as shown in Figure 7b), which should be sufficiently high higher than that of H₂S oxidation but lower than that of the OER, to oxidize H2S to elemental sulfur while avoiding excessive oxidation to generate by-products (SO₃²⁻, $S_2O_3^{2-}$ et al.). (2) The produced sulfur should be easily separable. (3) Both the oxidized and reduced states of the redox medium should be stable throughout the reaction and exhibit non-toxicity as well as environmental friendliness. Recently, many redox mediators such as $(VO_2)^+/(VO)^{2+}$, I^-/I_3^- , Fe^{2+}/Fe^{3+} and polyoxometalates $[Sm(PMo^{IV}O_{39})_2]^{11-}/[Sm(PMo^{V}O_{39})_2]^{55-}$ have been reported (Huang et al., 2009; Kim et al., 2014; Zhou et al., 2018; Zong et al., 2014).

3.2 Redox mediators for indirectly electrocatalytic decomposition of H₂S

3.2.1 Fe²⁺/Fe³⁺ as redox mediators

The Fe²⁺/Fe³⁺ (0.77 V vs. SHE) was the earliest employed as redox mediator for indirect electrocatalytic decomposition of H₂S to produce sulfur and hydrogen, owing to its cost-effectiveness, strong oxidative capability toward H2S, and facile electrochemical regeneration (Mizuta et al., 1991; Zhou et al., 2018). In 1991, Mizuta et al. first employed ferric chloride (FeCl₃) solution to oxidize H₂S, generating elemental sulfur, ferrous chloride (FeCl₂), and hydrochloric acid (HCl) (Mizuta et al., 1991). Subsequently, the electrolyte solution with FeCl2 and HCl after separating sulfur precipitate was introduced to the electrolysis system, where Fe²⁺ was oxidized to Fe3+ at the anode, while H+ was reduced at the cathode to produce hydrogen. Experimental results demonstrated that under conditions of 70 °C and an electrolysis voltage of 0.7 V, the absorption efficiency of H2S exceeded 99%. Huang et al. assembled a bipolar membrane electrolysis device using graphite cloth as the anode and platinum-coated graphite cloth as the cathode, with a proton exchange membrane for the electrochemical regeneration of Fe²⁺/Fe³⁺ in an indirect H₂S decomposition system (Huang et al., 2019). This bipolar



 6 Fe²⁺/Fe³⁺ as redox mediators for indirect electrocatalytic decomposition of H_2S . (a) Operating principle of the perovskite PV-EC H_2S splitting system (Ma et al., 2016). (b) Schematic illustration of the solar redox flow batteries design for indirectly driving H_2S splitting (Ma W. et al., 2019). (c) Stability test for H_2S splitting into hydrogen and sulfur with the off-field electrocatalysis system (Wang S. et al., 2024). (d) A schematic representation of the proposed liquid redox sulfur recovery process with EDTA ligands and fuel cell (Kim et al., 2013).

electrolysis device exhibited a compact structure and high electrolytic efficiency. Experimental results demonstrated that the current density varied with electrolytic voltage, temperature, and electrolyte composition. When [Fe3+] > 0.20 mol/L, the concentrations of Fe2+ and Fe3+ in the analyte showed no significant influence on the current density. Furthermore, Li's group constructed a perovskite photovoltaic-electrocatalytic (PV-EC) system for H₂S splitting by integrating a single perovskite solar cell, noble-metal-free catalysts and indirect decomposition of H₂S reaction (As shown in Figure 8a) (Ma et al., 2016). This established system achieved a solar-to-chemical energy conversion efficiency up to 13.5% during the PV-EC step. By employing Fe2+/Fe3+ as the redox mediator, 0.5 mol/L H₂SO₄ as the electrolyte, graphite carbon sheet as the catalyst for oxidation of mediators, and molybdenumtungsten phosphide (Mo-W-P) material as the cathode electrocatalyst for HER, the total energy consumption for producing an equivalent amount of hydrogen via H2S splitting was approximately 43.3% lower than that of conventional water splitting.

To further industrialize the indirect electrolysis of H_2S technology, Li's group has implemented modifications to conventional indirect electrolysis processes (Ma D. et al., 2019). They proposed an innovative concept for H_2S splitting that constructs a solar redox flow battery device based on Fe^{2+}/Fe^{3+} and H_4 [SiW₁₂VIO₄₀]/H₆ [SiW₁₀VIW₂VO₄₀] redox mediators and perovskite solar cells, which simultaneously stores/utilizes solar

energy via charge/discharge redox pairs while decomposing H₂S into hydrogen and elemental sulfur. As shown in Figure 8b, during the solar-driven charging, energy was stored in redox species by anodic oxidation of Fe^{2+} to Fe^{3+} and the coupled cathodic reduction of H_4 [SiW₁₂VIO₄₀] to H_6 [SiW₁₀VIW₂VO₄₀]. Subsequently, the stored chemical energy in the two redox couple pairs was discharged to realize hydrogen and sulfur production. Specifically, the charged Fe3+ anolyte was pumped into an absorption reactor to capture H2S and convert it into protons and elemental sulfur, whereas the charged H₆ [SiW₁₀VIW₂VO₄₀] and the protons were pumped into a catalytic hydrogen evolution reactor, which could enable efficient hydrogen production via heterogeneous catalysis with the cobalt phosphide (CoP) catalyst. The constructed flow battery system displayed the stabilized cell voltage at ~ 0.75 V during the long-term test and achieved a solar-tochemical energy conversion efficiency of 15.2%. Building on this foundation, Li's group further developed a solar redox flow battery system based on dual redox couples (Fe²⁺/Fe³⁺ and V³⁺/V²⁺), named as an electron-mediated off-field electrocatalysis approach of H₂S splitting, which realizes the laboratory scale-up (100 L_{H2S}/d) of electrochemical decomposition of H₂S (Wang Z. et al., 2024). This off-field electrocatalysis system could operatstably over 120 h for a capacity of 100 L_{H2S}/d H₂S, in which H₂S conversion efficiency is nearly 100%, sulfur-containing pollutant emissions are below 1 ppm, and the energy consumption for hydrogen evolution is estimated to be 2.8 kWh·Nm⁻³ H₂ (Figure 8c). This technology offers

(15)

a potential promise for the industrial application of electrocatalytic decomposition of H₂S.

In addition to the free Fe2+/Fe3+ redox species in acidic environments, the ethylenediaminetetraacetic acid (EDTA) ligands have been utilized to form iron complexes in alkaline conditions to capture H₂S and convert it into elemental sulfur, followed by electrochemical regeneration (as illustrated in Figure 8d) (Kim et al., 2013). And the absorption of H₂S is more favorable, and corrosivity is relatively weaker in alkaline conditions. The required energy input for driving the HER could be reduced due to the lower redox potential of Fe²⁺-EDTA/Fe³⁺-EDTA than that of free Fe²⁺/Fe³⁺ (0.77 V vs. SHE), thereby decreasing the overall energy consumption of H₂S splitting. Furthermore, the performance of the Fe²⁺-EDTA/Fe³⁺-EDTA redox couple is dramatically influenced by the pH value of the solution. When the pH value is 9, it can efficiently capture H2S and maximize the generation of electrical energy (Kim et al., 2013). The reaction equations for the process are as follows (Equations 15, 16):

Oxidation of H₂S:
$$2[Fe^{3+}\text{-EDTA}]^{-} + HS^{-} \rightarrow 2[Fe^{2+}\text{-EDTA}]^{2-} + H^{+} + S \downarrow$$

Anode:
$$2[Fe^{2+}-EDTA]^{2^{-}}-2e^{-} \rightarrow 2[Fe^{3+}-EDTA]^{-}$$
 (16)

3.2.2 I^-/I_3^- as redox mediators

The I^-/I_3^- with appropriate redox voltages (0.54 V vs. SHE) used as anodic redox mediator has been proven to facilitate selectively generating sulfur in the solution, effectively mitigating competitive sulfite/sulfate deposition on the electrode interface (Zong et al., 2014). Kalina et al. achieved the indirect electrocatalytic decomposition of H_2S into elemental sulfur and hydrogen in an acid environment (pH 0–1) by utilizing the I^-/I_3^- as redox mediators (Kalina, 1985). This redox pair displayed high solubility for both the reduced (I^-) and oxidized (I_3^-) forms with ideal stability, electrochemical activity, and relatively obstructed side reactions. The reaction equations for electrochemical H_2S splitting using the I^-/I_3^- redox are presented as follows (Equations 17–19):

Oxidation of
$$H_2S: I_3^- + H_2S \rightarrow 2H^+ + 3I^- + S \downarrow$$
 (17)

Anode:
$$3I^{-} - 2e^{-} \rightarrow I_{3}^{-}$$
 (18)

Cathode:
$$2H^+ + 2e^- \rightarrow H_2 \uparrow$$
 (19)

During the oxidation of H_2S , the generated sulfur is in the form of a reddish-brown viscous gel-like precipitate, and the sulfur purity is up to 90% after cooling. The sulfur recovery efficiency can reach 99.3% after treatment with hot toluene. Furthermore, Luo et al. constructed a self-driven photoelectrochemical splitting system of H_2S into elemental sulfur and hydrogen based on the I^-/I_3^- as redox mediators, a WO_3 photoanode and a Si/PVC photocathode (Figure 9a) (Luo et al., 2017). The system exhibited selective oxidation of H_2S to elemental sulfur without byproduct formation such as polysulfide (S_n^{-2}), attributable to the moderate oxidizing capability of I_3^- . Remarkably, high recovery rates of 1.04 mg h^{-1} cm⁻² for sulfur and 0.75 mL h^{-1} cm⁻² for hydrogen were achieved, demonstrating near-quantitative conversion of H_2S to these value-added products.

Moreover, for the indirectly electrocatalytic H_2S decomposition system, the electrochemical regeneration process with I^-/I_3^- as redox

mediators can not only couple with hydrogen evolution reaction to produce hydrogen, but also pair with Fe2+/Fe3+ redox couple for organic pollutant degradation. Additionally, it can be integrated with the oxygen reduction reaction to generate hydrogen peroxide (H₂O₂). For example, Li et al. proposed a photoelectrochemical approach for the synchronous recovery of sulfur from H₂S waste gas and removal of organic pollutants (carbamazepine) from wastewater driven by simulated solar light (Li et al., 2018). In this system, H₂S was selectively converted into high-purity elemental sulfur via the I⁻/ I₃ redox mediator at the photoanode, while carbamazepine pollutant was electrochemically oxidized and degraded at the cathode by Fe²⁺/Fe³⁺-activated peroxymonosulfate (Figure 9b). Notably, the sulfur recovery ratio reached 95.9% and the removal efficiency of carbamazepine pollutant was up to 91.6% within 1 h in this established system. In addition, Cui et al. designed an integrated gas-liquid flow electrocatalytic system to synergistically drive H2S oxidation on I⁻/I₃⁻ redox pairs and O₂ reduction on the catalyst surface, achieving simultaneous sulfur recovery and H2O2 production with low energy consumption (Figure 9c) (Cui et al., 2024). By implementing a dual-flow cell configuration integrating a carbon-supported gas diffusion electrode and an I⁻/I₃⁻ cyclic redox system, a high current density of 102 mA cm⁻² was achieved, and the corresponding yield rates for elemental sulfur and H2O2 reached 60 mg cm⁻² h⁻¹ and 50 mg cm⁻² h⁻¹, respectively.

3.2.3 Polyoxometalates as redox mediators

Recently, Polyoxometalates such as $PMo_{12}O_{40}^{3-}$ and $(NH_4)_{11}$ [Ln $(PMo_{11}O_{39})_2$] (Ln = Sm, Ce, Dy, or Gd) with appropriate redox potentials and chemical stability, have been used as redox media for efficiently indirect electrocatalytic oxidation of H_2S into sulfur and hydrogen production with a removing rate of over 90% under optimal conditions (Kim et al., 2014; Li Y. et al., 2021). The reaction equation of H_2S splitting by employing $[Sm(PMo_{11}^{VI}O_{39})_2]^{-11}/[Sm(PMo_{11}^{VI}O_{39})_2]^{-55}$ redox media as an example is as follows (Equations 20–22) (Kim and Lee, 2023; Li J. et al., 2021):

$$\begin{split} & \text{Oxidation of H_2S: } \left[\text{Sm} (\text{PMo}_{11}^{\text{VI}} \text{O}_{39})_2 \right]^{-11} \\ & + 22 \text{H}_2 \text{S} \rightarrow \left[\text{Sm} (\text{PMo}_{11}^{\text{VI}} \text{O}_{39})_2 \right]^{-55} + 44 \text{H}^+ + 22 \text{S} \downarrow \qquad (20) \\ & \text{Anode: } \left[\text{Sm} (\text{PMo}_{11}^{\text{VI}} \text{O}_{39})_2 \right]^{-55} - 44 \text{e}^- \rightarrow \left[\text{Sm} (\text{PMo}_{11}^{\text{VI}} \text{O}_{39})_2 \right]^{-11} \end{aligned} \tag{21}$$

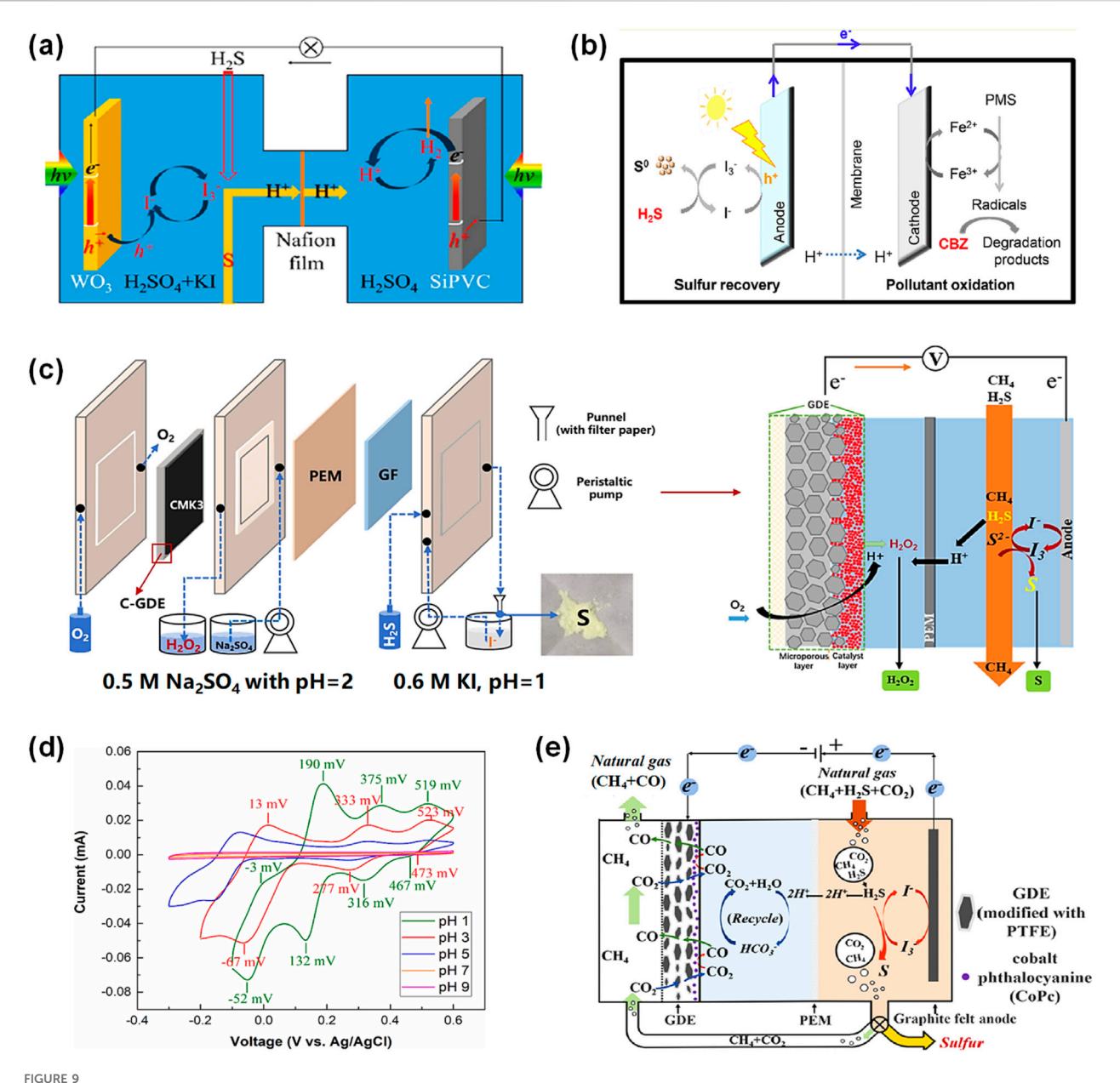
Cathode:
$$44H^+ + 44e^- \rightarrow 22H_2 \uparrow$$
 (22)

Research has demonstrated that the structure and performance of polyoxometalates are significantly influenced by the pH of the solution. The pH-dependent structural variations of polyoxometalates can be visually observed through color changes in the solution from dark yellow to light yellow to colorless. And the UV-vis spectrophotometry and Fourier transform infrared spectroscopy revealed the following transformations of polyoxometalates anions at different pH values (Equation 23) (Da Silva and Teixeira, 2017; Jürgensen and Moffat, 1995; Li J. et al., 2021):

$$[PMo_{12}O_{40}]^{3^{-}} \xrightarrow{pH > 1} [PMo_{11}O_{39}]^{7^{-}}$$

$$\xrightarrow{pH > 7} MoO_{4}^{2^{-}} + PO_{4}^{3^{-}}$$
(23)

Furthermore, the influence of pH on the structure and electrochemical performance of polyoxometalates was investigated



 I_1/I_3^- and polyoxometalates as redox mediators for indirect electrocatalytic decomposition of H_2S . (a) Schematic diagram of a self-driven photoelectrochemical splitting system of H_2S with I^-/I_3^- as redox mediator (Luo et al., 2017). (b) Schematic diagram of simultaneous recovery of sulfur resources from H_2S and degradation of organic pollutants by photoelectrocatalysis (Li et al., 2018). (c) The designed cell and operation mechanism for indirectly H_2S conversion to synchronously yield H_2O_2 and sulfur (Cui et al., 2024). (d) CV curves of 1 mM (NH₄)₁₁ [Sm(PMo₁₁O₃₉)₂] on a glassy carbon electrode at various pH values (Li J. et al., 2021). (e) Operation principle diagram for the electrocatalytic synergistic conversion of H_2S and CO_2 into sulfur and carbon monoxide system (Zhang B. et al., 2021).

by cyclic voltammetry (CV). The CV curves shown in Figure 9d indicated the redox peak intensities diminishing with increasing pH. At the lowest tested pH value (pH 1), the polyoxometalates existed in the Keggin structure, and the three largest consecutive redox peaks with each corresponding to a two-electron transfer process were observed, and this process can be illustrated by the following equations (Equation 24) (Lewera et al., 2005):

$$PMo_{12}^{VI}O_{40}^{3\text{-}} + nH^{\text{+}} + ne^{\text{-}} \rightarrow H_{n}PMo_{n}^{V}Mo_{12\text{--}n}^{VI}O_{40}^{3\text{-}} \tag{24} \label{eq:24}$$

where n is 2, 4, or 6. Further increasing the pH to 3 and 5, the Keggin structure of $PMo_{12}^{VI}O_{40}^{3-}$ transforms to lacunary-Keggin-

type $PMo_{11}^{VI}O_{39}^{7-}$, and three redox peaks with diminished current intensity were shown in the CV curves. These peaks can be explained by the following two-electron transfer processes (Equation 25) (Liu and Dong, 1994):

$$PMo_{11}^{VI}O_{39}^{7-} + nH^{+} + ne^{-} \rightarrow H_{n}PMo_{n}^{V}Mo_{11-n}^{VI}O_{39}^{7-}$$
 (25)

where n is 2, 4, or 6. When the pH was increased to >7, the redox peaks disappeared due to the decomposition of polyoxometalates. Therefore, the pH-dependent structure and redox activity of polyoxometalates were essential for electrochemically mediated H_2S capture and anodic regeneration. Additionally, the influence

of polyoxometalates concentration on H_2S removal efficiency was investigated (Kim et al., 2014). At pH 0.8, a lower polyoxometalates concentration (5 mM) resulted in less than 80% H_2S removal after 1 h, whereas a higher concentration (25 mM) maintained over 90% removal efficiency within 100 min. On the basis of the peak potentials observed in CV curves, it can be inferred that polyoxometalates oxidation at the anode coupled with hydrogen evolution at the cathode in the electrochemical regeneration unit occurred at potentials below 0.8–0.9 V (Kim and Lee, 2023).

3.2.4 Other redox mediators

The $(VO_2)^+/(VO)^{2+}$ with an oxidation potential of 0.99 V vs. SHE was also employed as redox media for indirect electrochemical oxidizing H_2S to elemental sulfur and regenerating at anode (Equations 26–28) (Huang et al., 2009).

Oxidation of
$$H_2S$$
: $(VO_2)^+ + 2H^+ + H_2S \rightarrow 2(VO)^{2+} + 2H_2O + S \downarrow$ (26)

Anode:
$$2(VO)^{2+} + 2H_2O - 2e^- \rightarrow 2(VO_2)^+ + 4H^+$$
 (27)

Cathode:
$$2H^+ + 2e^- \rightarrow H_2\#$$
 (28)

In the acidic vanadium oxo ion solution, the effects of absorption temperature, the molality of H^+ and $(VO)^{2+}$ in the electrolyte, as well as the molality of $(VO_2)^+$ in the absorption solution on both H_2S absorption efficiency and electrochemical decomposition efficiency were investigated. The results demonstrate that the H_2S absorption efficiency increases with rising absorption temperature. When the concentrations of H^+ and $(VO)^{2+}$ in the electrolyte reached 7.00 mol/kg and 0.65 mol/kg respectively, and the concentration of $(VO_2)^+$ in the absorption process was 0.55 mol/kg, the H_2S absorption efficiency exceeded 90% at 50 °C, while the current efficiency of the electrochemical regeneration process achieved 97% at 45 °C.

The indirect electrolysis method could decompose H_2S with different concentration ranges from low to high. By introducing redox mediators, this approach effectively mitigates sulfur passivation on electrodes. Currently, the indirect electrocatalytic splitting of H_2S process has demonstrated promising results in an expanded test of a certain scale. However, it still faces several challenges, including low mass transfer efficiency for oxidation of H_2S , corrosion of equipment by acidic electrolytes, mismatched reaction rates between chemical and electrochemical processes, difficulty in separating amorphous sulfur, and short lifespans of electrode materials. Therefore, the key to advancing this technology lies in developing long-lasting, high-performance, and low-cost electrode materials and electrolyzers, designing efficient redox mediators, optimizing process parameters, and improving sulfur recovery efficiency.

4 Conclusion and perspective

The electrochemical H_2S decomposition technology provides dual benefits of waste treatment and energy valorization, serving as an effective approach for achieving clean and high-value utilization of H_2S resources. In this review, we summarize recent progress in two key research directions: (1) Innovative strategies to mitigate anodic sulfur passivation in direct H_2S decomposition systems. (2) The development of redox mediators and process optimization for

indirect H₂S decomposition pathway. A comparative analysis of characteristic and reaction mechanism of both approaches is provided, with the aim of providing insights for the development of electrocatalytic H₂S decomposition technologies.

For the direct electrochemical decomposition of H₂S, these strategies such as organic solvent treatment, high-temperature melting technique, designing armored electrocatalyst, constructing sulfur-phobic electrocatalytic materials and modulating the anode products have been developed to solve the sulfur passivation at anode. However, the industrial application of this technology still faces several challenges, including the susceptibility of electrode materials to sulfurization at high current densities, poor material stability, and low sulfur recovery efficiency. Future development of this technology may focus on the following aspects: (1) Continuous exploitation of novel electrocatalytic materials with high activity and sulfur-passivation resistance. Transition metal sulfides/selenides are considered optimal choices for SOR catalysts due to their suitable adsorption energy for sulfur-containing species and excellent catalytic activity. High-entropy alloy compounds, with their highly tunable composition and structural advantages, also show great potential in SOR electrocatalysis. Constructing heterojunction catalysts could induce electron redistribution at the interface, generating synergistic effects, which serve as an effective strategy for developing SOR electrocatalysts. Additionally, with the rapid advancement of artificial intelligence in recent years, data-driven approaches such as high-throughput screening and machine learning have provided new research paradigms for the efficient design of SOR electrocatalysts. (2) In-depth understanding of the stability and distribution mechanisms of SOR products. By employing in situ characterization techniques to monitor the evolution of reactive intermediates and products (from polysulfides to sulfates) on the catalyst surface in real time, combined with theoretical calculations to elucidate the reaction pathway and mechanism, the sulfur precipitation behavior can be precisely regulated. Furthermore, achieving a single sulfur-containing product through targeted control of the SOR process is crucial for the resource utilization of sulfur, which is a key step toward the industrial application of this technology. (3) Optimization of electrocatalytic devices. High-efficiency electrocatalytic devices play a crucial role in enhancing the H₂S decomposition performance of the overall reaction system. Membrane electrode assembly (MEA)-based electrolyzers represent an ideal choice for future high-performance electrocatalytic devices, as they can significantly reduce the system impedance while maintaining the mass transport advantages of flow-type electrolyzers. Optimizing the design of electrolyzers and developing high-activity, low-cost and stable membrane electrodes are the development trends for MEA electrolyzers of H₂S high-efficiency decomposition to meet industrial requirements.

For the indirect electrochemical decomposition of H_2S , the sulfur passivation at the anode can be effectively mitigated by introducing redox couples as intermediate mediators. Various redox couples such as $(VO_2)^+/(VO)^{2+}$, I^-/I_3^- , Fe^{2+}/Fe^{3+} , and $[Sm(PMo^{IV}O_{39})_2]^{11-}/[Sm(PMo^{V}O_{39})_2]^{55-}$ have been developed, which enable efficient H_2S oxidation and electrochemical coupling for hydrogen production. Furthermore, the conventional indirect process has been optimized, leading to the proposal of an electron-mediated off-field electrocatalysis approach of H_2S splitting based on dual redox couples $(Fe^{2+}/Fe^{3+}$ and V^{3+}/V^{2+}), and this approach has demonstrated a promising result in a certain scale of expanded experiments. However, the indirect

electrolysis of H₂S still faces several challenges, including low mass transfer efficiency for H₂S oxidation, corrosion of equipment by acidic electrolytes, difficulty in separating amorphous sulfur, mismatched reaction rates between chemical and electrochemical processes and the short lifespan of electrode materials. Future research directions for this technology may focus on the following aspects: (1) Development of redox mediators with strong oxidizing capacity, high-purity sulfur production with easy separation, and low energy consumption for coupled hydrogen production. (2) Design of high-efficiency absorption reactors to enhance gas-liquid mass transfer and improve H₂S oxidation rate. (3) Exploitation of highly efficient and stable electrode materials. (4) Process optimization for indirect H₂S decomposition and development of advanced membrane electrode devices, such as coupling with oxygen reduction reaction to assemble fuel cells, thereby further reducing energy consumption of the process.

Additionally, in the processes of petroleum refining and natural gas purification, substantial carbon dioxide (CO2) is concomitantly released alongside H₂S. The conventional Claus process only purifies the harmful gas H2S and recovers sulfur, while neglecting the treatment of the greenhouse gas CO2, leading to hydrogen resource wastage and substantial carbon emissions. The electrocatalytic synergistic conversion of H2S and CO2 provides the potential to produce high-value products (e.g., sulfur, carbonic oxide, methane) under mild reaction conditions, which avoids the generation of byproducts such as carbonyl sulfide and sulfur dioxide, and simultaneously reduces carbon emissions (Fu et al., 2020; Ma et al., 2018; Zhang S. et al., 2021). For example, Zhang et al. constructed a system for the electrocatalytic synergistic conversion of H₂S and CO₂ into elemental sulfur and carbon monoxide (Figure 9E), utilizing the I⁻/I₃⁻ redox mediator and a gas diffusion electrode with polytetrafluoroethylene and cobalt phthalocyanine (CoPc) (Zhang B. et al., 2021). The system achieved production rates of 24.94 mg cm⁻²·h⁻¹ for elemental sulfur and 19.93 mL cm⁻²·h⁻¹ for carbon monoxide, respectively. Moreover, the model analysis revealed that the operational cost of simultaneous H₂S and CO₂ utilization in natural gas purification technology is marginally lower than that of solely utilizing H₂S. Therefore, the development of H₂S and CO2 co-conversion technology represents a promising future direction for natural gas purification, offering a sustainable pathway for resource utilization and emission reduction.

Author contributions

YC: Writing – review and editing, Investigation, Supervision, Conceptualization, Writing – original draft. MW: Supervision, Writing – review and editing. TD: Visualization, Writing – review and editing. RF: Funding acquisition,

References

Ai, L., Tian, Y., Xiao, T., Zhang, J., Zhang, C., and Jiang, J. (2024). Energy-saving hydrogen production from sulfion oxidation-hybrid seawater splitting enabled by superwettable corrosion-resistant NiFe layered double hydroxide/FeNi₂S₄ heterostructured nanoarrays. *J. Colloid Interface Sci.* 673, 607–615. doi:10.1016/j.jcis.2024.06.018

Ali, I., Imanova, G., Agayev, T., Aliyev, A., Jabarov, S., Albishri, H. M., et al. (2022). Seawater splitting for hydrogen generation using zirconium and its niobium alloy under gamma radiation. *Molecules* 27, 6325. doi:10.3390/molecules27196325

Writing – review and editing. QL: Writing – review and editing, Project administration. ZL: Writing – review and editing, Conceptualization. ZP: Writing – review and editing.

Funding

The author(s) declare that financial support was received for the research and/or publication of this article. The project was funded by the Postdoctoral Research Fund of Petrochina Southwest oil and Gasfield Company (no. 25XNYTSC021). The funder was not involved in the study design, collection, analysis, interpretation of data, the writing of this article, or the decision to submit it for publication.

Acknowledgements

The authors would like to acknowledge financial support from the Petrochina Southwest oil and Gasfield Company.

Conflict of interest

Authors YC, MW, TD, RF, QL, ZL, and ZP were employed by PetroChina Southwest Oil and Gasfield Company. Authors YC, MW, TD, QL, and ZL were employed by China National Petroleum Corporation.

Generative Al statement

The author(s) declare that no Generative AI was used in the creation of this manuscript.

Any alternative text (alt text) provided alongside figures in this article has been generated by Frontiers with the support of artificial intelligence and reasonable efforts have been made to ensure accuracy, including review by the authors wherever possible. If you identify any issues, please contact us.

Publisher's note

All claims expressed in this article are solely those of the authors and do not necessarily represent those of their affiliated organizations, or those of the publisher, the editors and the reviewers. Any product that may be evaluated in this article, or claim that may be made by its manufacturer, is not guaranteed or endorsed by the publisher.

Anani, A. A., Mao, Z., White, R. E., Srinivasan, S., and Appleby, A. J. (1990). Electrochemical production of hydrogen and sulfur by low-temperature decomposition of hydrogen sulfide in an aqueous alkaline solution. *J. Electrochem. Soc.* 137, 2703–2709. doi:10.1149/1.2087021

Ateya, B. G., Alkharafi, F. M., and Al-Azab, A. S. (2003). Electrodeposition of sulfur from sulfide contaminated brines. *Electrochem. Solid-State Lett.* 6, C137. doi:10.1149/1. 1599686

- Basheer, A. A., and Ali, I. (2019). Water photo splitting for green hydrogen energy by green nanoparticles. *Int. J. Hydrogen Energy* 44, 11564–11573. doi:10.1016/j.ijhydene. 2019.03.040
- Chen, J., Xu, W., Zhu, J., Wang, X., and Zhou, J. (2020). Highly effective direct decomposition of H₂S by microwave catalysis on core-shell Mo₂N-MoC@SiO₂ microwave catalyst. *Appl. Catal. B Environ.* 268, 118454. doi:10.1016/j.apcatb.2019. 118454
- Chuang, K. T., Donini, J. C., Sanger, A. R., and Slavov, S. V. (2000). A proton-conducting solid state $H_2S\pm O_2$ fuel cell. *Int. J. Hydrogen Energy* 25. doi:10.1016/s0360-3199(98)00003-2
- Cui, H., Zhou, C., Zhang, Y., Zhou, T., Xie, C., Li, L., et al. (2024). Highly-efficient natural gas desulfurization and simultaneous H₂O₂ synthesis based on the electrochemical coupling reaction strategy. *J. Hazard Mater* 463, 132823. doi:10. 1016/j.jhazmat.2023.132823
- Da Silva, M. J., and Teixeira, M. G. (2017). An unexpected behavior of ${\rm H_3PMo_{12}O_{40}}$ heteropolyacid catalyst on the biphasic hydrolysis of vegetable oils. *RSC Adv.* 7, 8192–8199. doi:10.1039/C6RA27287H
- De Crisci, A. G., Moniri, A., and Xu, Y. (2019). Hydrogen from hydrogen sulfide: towards a more sustainable hydrogen economy. *Int. J. Hydrogen Energy* 44, 1299–1327. doi:10.1016/j.ijhydene.2018.10.035
- Duan, C., Tang, C., Yu, S., Li, L., Li, J., and Zhou, Y. (2023). Efficient electrocatalytic desulfuration and synchronous hydrogen evolution from H₂S *via* anti-sulfuretted NiSe nanowire array catalyst. *Appl. Catal. B Environ.* 324, 122255. doi:10.1016/j.apcatb.2022. 122255
- Duan, C., Tang, C., Du, Y., Yu, S., Guo, H., Bai, Y., et al. (2024). Direct solar-driven electrochemical dissociation of $\rm H_2S$ to $\rm H_2$ with 12 % solar-to-hydrogen conversion efficiency in diaphragm electrolytic reactor. *Appl. Catal. B Environ. Energy* 355, 124146. doi:10.1016/j.apcatb.2024.124146
- Eow, J. S. (2002). Recovery of sulfur from sour acid gas: a review of the technology. *Environ. Prog.* 21, 143–162. doi:10.1002/ep.670210312
- Fu, X. Z., Li, J., Pan, X. R., Huang, L., Li, C. X., Cui, S., et al. (2020). A single microbial electrochemical system for CO₂ reduction and simultaneous biogas purification, upgrading and sulfur recovery. *Bioresour. Technol.* 297, 122448. doi:10.1016/j. biortech.2019.122448
- Garg, K., Kumar, M., Kaur, S., and Nagaiah, T. C. (2023). Electrochemical production of hydrogen from hydrogen sulfide using cobalt cadmium sulfide. *ACS Appl. Mater. Interfaces* 15, 27845–27852. doi:10.1021/acsami.3c01318
- Huang, H., Yu, Y., and Chung, K. H. (2009). Recovery of hydrogen and sulfur by indirect electrolysis of hydrogen sulfide. *Energy and Fuels* 23, 4420–4425. doi:10.1021/ef900424a
- Huang, H., Shang, J., Yu, Y., and Chung, K. H. (2019). Recovery of hydrogen from hydrogen sulfide by indirect electrolysis process. *Int. J. Hydrogen Energy* 44, 5108–5113. doi:10.1016/j.ijhydene.2018.11.010
- Huo, J., Jin, L., Chen, C., Chen, D., Xu, Z., Wilfred, C. D., et al. (2023). Improving the sulfurophobicity of the NiS-Doping CoS electrocatalyst boosts the low-energy-consumption sulfide oxidation reaction process. ACS Appl. Mater Interfaces 15, 43976–43984. doi:10.1021/acsami.3c11602
- Ipsakis, D., Kraia, T., Marnellos, G. E., Ouzounidou, M., Voutetakis, S., Dittmeyer, R., et al. (2015). An electrocatalytic membrane-assisted process for hydrogen production from H 2 S in black sea: preliminary results. *Int. J. Hydrogen Energy* 40, 7530–7538. doi:10.1016/j.ijhydene.2014.12.017
- Jin, L., Chen, C., Hu, L., Liu, X., Ding, Y., He, J., et al. (2022). Ligand-induced electronic structure and morphology regulation in $\mathrm{Ni}_3\mathrm{S}_2$ heterostructures for efficient bifunctional electrocatalysis. *Appl. Surf. Sci.* 605, 154756. doi:10.1016/j.apsusc.2022.154756
- Jürgensen, A., and Moffat, J. B. (1995). The stability of 12-molybdosilicic, 12-tungstosilicic, 12-molybdophosphoric and 12-tungstophosphoric acids in aqueous solution at various pH. *Catal. Lett.* 34, 237–244. doi:10.1007/BF00808338
- Kalina, D. W., and Maasjr, E. (1985). Indirect hydrogen sulfide conversion—I. An acidic electrochemical process. *Int. J. Hydrogen Energy* 10, 157–162. doi:10.1016/0360-3199(85)90022-9
- Khabazipour, M., and Anbia, M. (2019). Removal of hydrogen sulfide from gas streams using porous materials: a review. *Industrial and Eng. Chem. Res.* 58, 22133–22164. doi:10.1021/acs.iecr.9b03800
- Kim, K., and Lee, C. (2023). Recent progress in electrochemical hydrogen sulfide splitting: strategies for enabling Sulfur-tolerant anodic reactions. *Chem. Eng. J.* 469, 143861. doi:10.1016/j.cej.2023.143861
- Kim, K., Kim, D. Y., Lee, K. R., and Han, J.-I. (2013). Electricity generation from iron EDTA-based liquid redox sulfur recovery process with enhanced stability of EDTA. *Energy Convers. Manag.* 76, 342–346. doi:10.1016/j.enconman.2013.07.063
- Kim, K., Song, D., and Han, J.-I. (2014). A liquid redox sulfur recovery process based on heteropoly molybdophosphate (HPMo) with electricity generation. *Chem. Eng. J.* 241, 60–65. doi:10.1016/j.cej.2013.12.007
- Lewera, A., Chojak, M., Miecznikowski, K., and Kulesza, P. J. (2005). Identification and electroanalytical characterization of redox transitions in solid-state keggin type phosphomolybdic acid. *Electroanalysis* 17, 1471–1476. doi:10.1002/elan.200503295

- Li, J., Chen, C.-B., Wang, D.-D., Li, C.-X., Zhang, F., Li, D.-B., et al. (2018). Solar-Driven synchronous photoelectrochemical sulfur recovery and pollutant degradation. *ACS Sustain. Chem. and Eng.* 6, 9591–9595. doi:10.1021/acssuschemeng.8b02678
- Li, J., Wang, R., and Dou, S. (2021a). Electrolytic cell-assisted polyoxometalate based redox mediator for H₂S conversion to elemental sulphur and hydrogen. *Chem. Eng. J.* 404, 127090. doi:10.1016/j.cej.2020.127090
- Li, Y., Bahamon, D., Sinnokrot, M., Al-Ali, K., Palmisano, G., and Vega, L. F. (2021b). Computational modeling of green hydrogen generation from photocatalytic H₂S splitting: overview and perspectives. *J. Photochem. Photobiol. C Photochem. Rev.* 49, 100456. doi:10.1016/j.jphotochemrev.2021.100456
- Li, M., Dong, X., Gao, P., Yin, L., Chen, G., Gao, P., et al. (2024). The crucial role of nMOFs in $\rm H_2S$ absorption process using ionic liquid solution based nanofluid systems. *Chem. Eng. J.* 480, 148072. doi:10.1016/j.cej.2023.148072
- Liu, M., and Dong, S. (1994). Electrochemical behavior of molibdosilicic heteropoly complex with dysprosium and its doped polypyrrole film modified electrode. *Electrochimica Acta* 40, 197–200. doi:10.1016/0013-4686(94)00294-b
- Liu, M., He, P., Luo, J. L., Sanger, A. R., and Chuang, K. T. (2001). Performance of a solid oxide fuel cell utilizing hydrogen sulfide as fuel. *J. Power Source* 94, 20–25. doi:10. 1016/s0378-7753(00)00660-1
- Luo, T., Bai, J., Li, J., Zeng, Q., Ji, Y., Qiao, L., et al. (2017). Self-Driven photoelectrochemical splitting of H₂S for S and H₂ recovery and simultaneous electricity generation. *Environ. Sci. Technol.* 51, 12965–12971. doi:10.1021/acs.est.7b03116
- Ma, W., Han, J., Yu, W., Yang, D., Wang, H., Zong, X., et al. (2016). Integrating perovskite photovoltaics and noble-metal-free catalysts toward efficient solar energy conversion and H₂S splitting. ACS Catal. 6, 6198–6206. doi:10.1021/acscatal.6b01772
- Ma, Y., Liu, X., and Wang, R. (2017). Efficient removal of $\rm H_2S$ at high temperature using the ionic liquid solutions of [C4mim]₄PMo₁₂O₄₀-An organic polyoxometalate. *J. Hazard Mater* 331, 109–116. doi:10.1016/j.jhazmat.2017.02.036
- Ma, W., Wang, H., Yu, W., Wang, X., Xu, Z., Zong, X., et al. (2018). Achieving simultaneous $\rm CO_2$ and $\rm H_2S$ conversion via a coupled Solar-Driven electrochemical approach on non-precious-metal catalysts. *Angew. Chem. Int. Ed.* 57, 3473–3477. doi:10. 1002/anie.201713029
- Ma, D., Hu, B., Wu, W., Liu, X., Zai, J., Shu, C., et al. (2019a). Highly active nanostructured CoS₂/CoS heterojunction electrocatalysts for aqueous polysulfide/iodide redox flow batteries. *Nat. Commun.* 10, 3367. doi:10.1038/s41467-019-11176-y
- Ma, W., Xie, C., Wang, X., Wang, H., Jiang, X., Zhang, H., et al. (2019b). High-Performance solar redox flow battery toward efficient overall splitting of hydrogen sulfide. *ACS Energy Lett.* 5, 597–603. doi:10.1021/acsenergylett.9b02206
- Ma, Y., Jin, X., Hu, Y., Huang, Q., and Wang, Z. (2020). Recovery of hydrogen and sulfur by electrolysis of ionized H₂S in an amine-containing organic electrolyte with highly temperature-dependent sulfur solubility. *Energy and Fuels* 34, 7756–7762. doi:10.1021/acs.energyfuels.0c01161
- Mbah, J., Srinivasan, S., Krakow, B., Wolan, J., Goswami, Y., Stefanakos, E., et al. (2010). Effect of RuO₂–CoS₂ anode nanostructured on performance of H₂S electrolytic splitting system. *Int. J. Hydrogen Energy* 35, 10094–10101. doi:10.1016/j.ijhydene.2010.
- Mizuta, S., Kondo, W., Fujii, K., Iida, H., Isshiki, S., Noguchi, H., et al. (1991). Hydrogen production from hydrogen sulfide by the iron-chlorine hybrid process. *Industrial and Eng. Chem. Res.* 30, 1601–1608. doi:10.1021/ie00055a028
- Oladipo, H., Yusuf, A., Al Jitan, S., and Palmisano, G. (2021). Overview and challenges of the photolytic and photocatalytic splitting of $\rm H_2S$. *Catal. Today* 380, 125–137. doi:10. 1016/j.cattod.2021.03.021
- Osasuyi, O., Quang, D. V., Basina, G., Al Wahedi, Y., Abu Zahra, M. R. M., Palmisano, G., et al. (2022). Reversible metal sulfide transition in a two-step thermochemical H₂S splitting. *Industrial and Eng. Chem. Res.* 61, 6135–6145. doi:10.1021/acs.iecr.1c02569
- Pei, Y., Cheng, J., Zhong, H., Pi, Z., Zhao, Y., and Jin, F. (2021). Sulfide-oxidation-assisted electrochemical water splitting for $\rm H_2$ production on a bifunctional $\rm Cu_2S/nickel$ foam catalyst. *Green Chem.* 23, 6975–6983. doi:10.1039/d1gc01857d
- Pei, Y., Li, D., Qiu, C., Yan, L., Li, Z., Yu, Z., et al. (2024). High-entropy sulfide catalyst boosts energy-saving electrochemical sulfion upgrading to thiosulfate coupled with hydrogen production. *Angew. Chem. Int. Ed. Engl.* 63, e202411977. doi:10.1002/anie.
- Sassi, M., and Amira, N. (2012). Chemical reactor network modeling of a microwave plasma thermal decomposition of $\rm H_2S$ into hydrogen and sulfur. *Int. J. Hydrogen Energy* 37, 10010–10019. doi:10.1016/j.ijhydene.2012.04.006
- Semwal, S., Shakir, R., Karthikeyan, J., Sinha, A. S. K., and Ojha, U. (2023). NiFeOOH-Co $_9S_8$ -Intercalated nanostructure arrays for energy-efficient H2 production and sulfion oxidation at high Current density. *ACS Appl. Nano Mater.* 6, 18945–18956. doi:10.1021/acsanm.3c03438
- Sezer, N., Khalid, F., Biçer, Y., and Koç, M. (2020). Electrochemical modeling and performance assessment of H₂S/Air solid oxide fuel cell. *Energy Technol.* 8, 2000531. doi:10.1002/ente.202000531
- Shih, Y. S. L. J. L., and Lee, J. L. (1986). Continuous solvent extraction of sulfur from the electrochemical oxidation of a basic sulfide solution in the CSTER System. *Ind. Eng. Chem. Process Des. Dev.* 25, 834–836. doi:10.1021/i200034a041

Wang, Y., Liu, X., Kraslawski, A., Gao, J., and Cui, P. (2019). A novel process design for CO_2 capture and H_2S removal from the syngas using ionic liquid. *J. Clean. Prod.* 213, 480–490. doi:10.1016/j.jclepro.2018.12.180

- Wang, S., Rohani, V., Leroux, P., Gracian, C., Nastasi, V., and Fulcheri, L. (2024a). Progress on hydrogen sulfide removal: from catalytic oxidation to plasma-assisted treatment. *Chemosphere* 364, 143174. doi:10.1016/j.chemosphere.2024.143174
- Wang, Z., Wang, Q. N., Ma, W., Liu, T., Zhang, W., Zhou, P., et al. (2024b). Hydrogen sulfide splitting into hydrogen and sulfur through off-field electrocatalysis. *Environ. Sci. Technol.* 58, 10515–10523. doi:10.1021/acs.est.4c00312
- Wei, J., and Wu, X. (2025). Self-Powered water electrolysis with sulfide waste as consumable. ACS Sustain. Chem. and Eng. 13, 2913–2923. doi:10.1021/acssuschemeng.
- Yang, J., Smulders, V., Smits, J. J. T., Mei, B. T., and Mul, G. (2019). Electrochemical oxidation of H_2S on polycrystalline Ni electrodes. *J. Appl. Electrochem.* 49, 929–936. doi:10.1007/s10800-019-01334-x
- Yang, H., Bai, J., Zhou, T., Zhou, C., Xie, C., Zhang, Y., et al. (2023). Electrochemical coupling conversion of sulfur-containing gaseous waste to treasure: a key review. *Appl. Catal. A General* 654, 119085. doi:10.1016/j.apcata.2023.119085
- Yang, T., Liu, M., Wang, M., Shi, Y., Liu, F., and Zhao, T. (2025). Phenolic-amine protic ionic liquids with multiple active sites for the selective absorption and conversion of $\rm H_2S$. *J. Environ. Chem. Eng.* 13, 117597. doi:10.1016/j.jece.2025.117597
- Yates, C., and Winnick, J. (1999). Anode materials for a hydrogen sulfide solid oxide fuel cell. J. Electrochem. Soc. 146, 2841–2844. doi:10.1149/1.1392017
- Yi, L., Ji, Y., Shao, P., Chen, J., Li, J., Li, H., et al. (2021). Scalable synthesis of tungsten disulfide nanosheets for alkali-acid electrocatalytic sulfion recycling and $\rm H_2$ generation. Angew. Chem. Int. Ed. Engl. 60, 21550–21557. doi:10.1002/anie.202108992
- Yu, W., Yu, J., Wang, Y., Li, X., Wang, Y., Yuan, H., et al. (2022). Electrocatalytic upcycling of nitrate and hydrogen sulfide *via* a nitrogen-doped carbon nanotubes encapsulated iron carbide electrode. *Appl. Catal. B Environ.* 310, 121291. doi:10.1016/j.apcatb.2022.121291
- Yu, Z., Deng, Z., Li, Y., and Wang, X. (2024). Advances in electrocatalyst design and mechanism for sulfide oxidation reaction in hydrogen sulfide splitting. *Adv. Funct. Mater.* 34, 2403435. doi:10.1002/adfm.202403435
- Zhang, W., Lei, D., and Feng, W. (2014). An approach for estimating toxic releases of $\rm H_2S$ -containing natural gas. *J. Hazard Mater* 264, 350–362. doi:10.1016/j.jhazmat.2013. 09.070

- Zhang, X., Tang, Y., Qu, S., Da, J., and Hao, Z. (2015). H2S-Selective catalytic oxidation: catalysts and processes. ACS Catal. 5, 1053–1067. doi:10.1021/cs501476p
- Zhang, M., Guan, J., Tu, Y., Chen, S., Wang, Y., Wang, S., et al. (2020). Highly efficient H_2 production from H_2 S via a robust graphene-encapsulated metal catalyst. *Energy and Environ. Sci.* 13, 119–126. doi:10.1039/c9ee03231b
- Zhang, B., Bai, J., Zhang, Y., Zhou, C., Wang, P., Zha, L., et al. (2021a). High yield of CO and synchronous S recovery from the Conversion of CO₂ and H₂S in natural gas based on a novel electrochemical reactor. *Environ. Sci. Technol.* 55, 14854–14862. doi:10. 1021/acs.est.1c04414
- Zhang, S., Zhou, Q., Shen, Z., Jin, X., Zhang, Y., Shi, M., et al. (2021b). Sulfophobic and vacancy design enables self-cleaning electrodes for efficient desulfurization and concurrent hydrogen evolution with low energy consumption. *Adv. Funct. Mater.* 31, 2101922. doi:10.1002/adfm.202101922
- Zhang, L., Wang, Z., and Qiu, J. (2022). Energy-Saving hydrogen production by seawater electrolysis coupling sulfion degradation. *Adv. Mater.* 34, e2109321. doi:10.1002/adma.202109321
- Zhang, B., Song, Z., Pang, Y., Zhang, X., Zhang, J., Mao, Y., et al. (2024). Tungstenneedle intensifies microwave-sustained plasma accelerating direct H₂S conversion to H₂. J. Hazard Mater 478, 135487. doi:10.1016/j.jhazmat.2024.135487
- Zhang, M., Wang, Z., Jiang, L., Bo, X., Cui, X., and Deng, D. (2025). Highly effective and durable integrated-chainmail electrode for $\rm H_2$ production through $\rm H_2S$ electrolysis. Angew. Chem. Int. Ed. Engl. 64, e202502032. doi:10.1002/anie.202502032
- Zhao, W., Manno, M., Al Wahedi, Y., Tsapatsis, M., and Stein, A. (2021). Regenerable sorbent pellets for the removal of Dilute H₂S from claus process tail gas. *Industrial and Eng. Chem. Res.* 60, 18443–18451. doi:10.1021/acs.iecr.1c03738
- Zheng, X., Lei, G., Wang, S., Shen, L., Zhan, Y., and Jiang, L. (2023). Advances in resources recovery of $\rm H_2S$: a review of desulfurization processes and catalysts. *ACS Catal.* 13, 11723–11752. doi:10.1021/acscatal.3c02294
- Zhou, Q., Shen, Z., Zhu, C., Li, J., Ding, Z., Wang, P., et al. (2018). Nitrogen-Doped CoP electrocatalysts for coupled hydrogen evolution and sulfur generation with low energy consumption. *Adv. Mater.* 30, 1800140. doi:10.1002/adma.201800140
- Zong, X., Han, J., Seger, B., Chen, H., Lu, G. M., Li, C., et al. (2014). An integrated photoelectrochemical-chemical loop for solar-driven overall splitting of hydrogen sulfide. *Angew. Chem. Int. Ed. Engl.* 53, 4399–4403. doi:10.1002/anie.201400571